

ORIGINAL ARTICLE

Selective Inactivation of Reelin in Inhibitory Interneurons Leads to Subtle Changes in the Dentate Gyrus But Leaves Cortical Layering and Behavior Unaffected

Jasmine Pahle¹, Mary Muhia², Robin J. Wagener³, Anja Tippmann^{1,4}, Hans H. Bock⁵, Janice Graw⁶, Joachim Herz⁷, Jochen F. Staiger⁸, Alexander Drakew^{1,9}, Matthias Kneussel², Gabriele M. Rune⁶, Michael Frotscher^{1,†} and Bianka Brunne^{1,6}

¹Institute for Structural Neurobiology, Center for Molecular Neurobiology, ZMNH, University Medical Center Hamburg-Eppendorf, 20251 Hamburg, Germany, ²Institute of Molecular Neurogenetics, Center for Molecular Neurobiology, ZMNH, University Medical Center Hamburg-Eppendorf, 20251 Hamburg, Germany, ³Neurology Clinic, University Hospital Heidelberg, Im Neuenheimer Feld 400, 69120 Heidelberg, Germany, ⁴Department of Systems Neuroscience, Johann-Friedrich-Blumenbach Institute for Zoology and Anthropology, University of Göttingen, 37075 Göttingen, Germany, ⁵Clinic of Gastroenterology and Hepatology, Heinrich-Heine-University Düsseldorf, 40225 Düsseldorf, Germany, ⁶Institute of Neuroanatomy, University Medical Center Hamburg-Eppendorf, 20251 Hamburg, Germany, ⁷Department of Molecular Genetics, University of Texas Southwestern Medical Center, Dallas, TX 75390, USA, ⁸Institute for Neuroanatomy, University Medical Center Göttingen, Georg-August-University Göttingen, 37075 Göttingen, Germany, and ⁹Institute of Clinical Neuroanatomy, Faculty of Medicine, 60590 Frankfurt, Germany

Address correspondence to Dr Bianka Brunne, Institute of Neuroanatomy, University Medical Center Hamburg, Martinistr. 52, 20246 Hamburg, Germany. Email: bbrunne@uke.de.

†Deceased

M.F. and B.B. contributed equally to this work

Abstract

Reelin is an extracellular matrix protein, known for its dual role in neuronal migration during brain development and in synaptic plasticity at adult stages. During the perinatal phase, Reelin expression switches from Cajal-Retzius (CR) cells, its main source before birth, to inhibitory interneurons (IN), the main source of Reelin in the adult forebrain. IN-derived Reelin has been associated with schizophrenia and temporal lobe epilepsy; however, the functional role of Reelin from INs is presently unclear. In this study, we used conditional knockout mice, which lack Reelin expression specifically in inhibitory INs, leading to a substantial reduction in total Reelin expression in the neocortex and dentate gyrus. Our results show that IN-specific Reelin knockout mice exhibit normal neuronal layering and normal behavior, including spatial reference

memory. Although INs are the major source of Reelin within the adult stem cell niche, Reelin from INs does not contribute substantially to normal adult neurogenesis. While a closer look at the dentate gyrus revealed some unexpected alterations at the cellular level, including an increase in the number of Reelin expressing CR cells, overall our data suggest that Reelin derived from INs is less critical for cortex development and function than Reelin expressed by CR cells.

Key words: adult neurogenesis, Calretinin, CB1, GFAP

Introduction

The *reeler* mutant mouse, deficient in Reelin, has provided major insights into the development of laminated brain structures (Falconer 1951; D'Arcangelo et al. 1995; reviewed by Rakic and Caviness 1995; Tissir and Goffinet 2003; D'Arcangelo 2006) where Reelin, synthesized by Cajal-Retzius (CR) cells of the forebrain, is essential. Reelin is a large extracellular glycoprotein involved in complex signaling mechanisms during neuronal migration, which are related to cytoskeletal dynamics and cell–cell, as well as cell–matrix adhesion (reviewed by Sekine et al. 2014; Bock and May 2016; Lee and D'Arcangelo 2016). CR cells, which are an early embryonic source of Reelin, are located beneath the pial surface of the cortex and olfactory bulb, as well as at the outer border of the dentate gyrus. They already start to express Reelin at E11.5 during their migration from their diverse origins in the developing pallium, including the cortical hem, to their final position below the meninges of the cortex (Takiguchi-Hayashi et al. 2004; Bielle et al. 2005). Reelin expression in CR cells remains high throughout the developmental stages of the neocortex (NC) and hippocampus (HC), but shortly after birth the number of Reelin-expressing CR cells decreases rapidly until postnatal day 20 (Ikeda and Terashima 1997; Schiffmann et al. 1997)—this is connected to a general decrease in CR cell numbers during this period (Anstötz et al. 2016). Reciprocal to the decline in the number of Reelin-expressing CR cells, inhibitory interneurons (IN) start to express Reelin and increase their Reelin expression (Alcantara et al. 1998; Pesold et al. 1998). Inhibitory INs are a heterogeneous cell population and only a subset of them expresses Reelin. This is well documented in the somatosensory barrel cortex where about 40% of all INs express Reelin. These Reelin-expressing INs are widely distributed throughout the NC, belong to different IN subpopulations (Pesold et al. 1999; Pohlkamp et al. 2014; Tasic et al. 2018), and arise from both the medial and caudal ganglionic eminence (Miyoshi et al. 2010). Like CR cells, these GABAergic INs have been shown to secrete Reelin to affect cells in their vicinity (Campo et al. 2009).

The specific function of this additional source of Reelin is presently unclear; however, it has been proposed that it contributes to the pathogenesis of brain disorders. Several laboratories have reported reduced Reelin levels in the post-mortem brains of schizophrenic patients (Impagnatiello et al. 1998; Fatemi et al. 2000; Guidotti et al. 2000; reviewed by Fatemi 2001 and Costa et al. 2002). In temporal lobe epilepsy (TLE), a loss of Reelin-expressing INs in the hilar region is associated with dentate gyrus granule cell dispersion (Haas and Frotscher 2009; Müller et al. 2009; Tinnes et al. 2013, Orcinha et al. 2016).

In this study, we addressed whether, and how a cell-type specific depletion of Reelin protein expression in INs may affect the developing and/or the adult brain. To this end, we crossbred a mouse line with loxP sites flanking the first Reelin exon (Lane-Donovan et al. 2015) with a mouse line expressing Cre recombinase under the *Dlx5/6* promoter (Monory et al. 2006), known to selectively target INs emerging from the ganglionic eminences during early embryonic development. The early activity of the

Dlx5/6 promoter, starting from E9.5 in the primordium of the ganglionic eminence in mice (Simeone et al. 1994; Hevner et al. 2003), will lead to Cre-mediated inactivation of the *reelin* gene in inhibitory INs several days prior to its physiological expression in these cells, which starts between postnatal day 0 (P0) and P5 in wild-type mice (Alcantara et al. 1998; Pesold et al. 1998).

This study mainly focused on the dentate gyrus, where several specific aspects of Reelin function in the adult brain have been proposed; namely, the stabilization of the granule cell layer (Haas and Frotscher 2009; Müller et al. 2009; Tinnes et al. 2013, Orcinha et al. 2016) and regulation of adult neurogenesis in the subgranular zone (SGZ; Won et al. 2006; Zhao et al. 2007; Sibbe et al. 2015). Based on our results, it appears unlikely that IN-derived Reelin substantially contributes to these aspects of Reelin function in the adult dentate gyrus. Extended analyses of neocortical layering and general behavior did not reveal any consequences of IN-specific Reelin loss on brain development and function, including learning and memory.

However, we identified several unexpected changes in the dentate gyrus of IN-specific Reelin knockout mice, namely 1) an upregulation of Calretinin and Cannabinoid receptor type 1 (CB1) levels in the inner molecular layer (iML) and 2) a decrease of glial fibrillary acidic protein (GFAP) filaments in astrocytes. Interestingly, we also identified an increase in the number of Reelin-expressing CR cells at the hippocampal fissure.

Material and Methods

Animals

All mouse strains were maintained on a C57Bl6/J background. Backcrossing was performed at least every third generation. The mice were housed under standard conditions, with food and water provided ad libitum. Experiments were conducted in accordance with the German and European Union laws on protection of experimental animals following approval by the local authorities of the City of Hamburg (Committee for Lebensmittelsicherheit und Veterinärwesen, Authority of Soziales, Familie, Gesundheit und Verbraucherschutz Hamburg, Germany, No. G14/111, Org 604 and Org 850). The animals were sacrificed at different ages: postnatal day (P) 3, 6, 10, and 21 and postnatal week (w) 8, 15, 20, 24, and 30.

The following mouse lines were used in this study: conditional Reelin mice with the first Reelin exon flanked by loxP sites (Lane-Donovan et al. 2015)—referred to as *Re^{fl/fl}*; Tg (*dlx5a-Cre*)1Mekk/J mice, expressing Cre recombinase during early embryonic development in inhibitory INs originating from the ganglionic eminences under the control of the *Dlx5/6* promoter (Monory et al. 2006)—referred to as *Dlx5/6-Cre*; B6.C-Tg (CMV-Cre)1Cgn/J mice (Schwenk et al. 1995), expressing Cre recombinase under the ubiquitously expressed CMV promoter—referred to as CMV-Cre (breeding of these CMV-Cre line with the *Re^{fl/fl}* line leads to an inheritable deletion of the first Reelin exon; the resulting animals are referred to as *Re^{dl/dl}*); reporter mice R26tdRFP, containing a Cre-inducible tandem-dimer

red fluorescent protein (tdRFP) within the ubiquitously expressed ROSA26 locus (Luche et al. 2007) – referred to as tdRFP reporter; Tg (Thy1-EGFP)*MJrs/J* mice expressing eGFP under the Thy1 promoter in a subpopulation of mature neurons (Feng et al. 2000) – referred to as Thy1eGFP; POMCeGFP mice expressing eGFP in immature granule cells of the dentate gyrus under the control of the proopiomelanocortin (POMC) promoter (Overstreet et al. 2004).

BrdU Administration

In a first approach, 12-week-old mice (five animals per group) received a single intraperitoneal injection of 50 µg/g body weight of 5-bromo-2-deoxyuridine (BrdU; Sigma-Aldrich) in 0.9% NaCl. The tissue was collected for immunohistochemistry (IHC) 21 days after the BrdU injection (age: 15 weeks). In a second approach, the mice received 1 mg/ml BrdU with their drinking water (supplemented with 1% sucrose) for 2 weeks (age: 11 weeks at the onset of the BrdU administration, seven animals per group). The tissue was collected for IHC 28 days after the first day of BrdU administration (age: 15 weeks).

Immunohistochemistry

IHC was performed as described previously (Brunne et al. 2010). In brief, mice were perfused with 0.01 M phosphate-buffered saline pH 7.4 (PBS) and brains were immersion-fixed in 4% paraformaldehyde in PBS pH 7.4 for 48 h at 4°C. Serial coronal or sagittal sections of 50 µm thickness were obtained using a Leica Vibratome VT 1000S. The following antibodies were used as primary antibodies: mouse anti-Reelin (Merck-Millipore MAB5364, 1:500); mouse anti-NeuN (Merck-Millipore MAB377, 1:1000); rabbit anti-Ki-67 (Thermo Fisher RM-9106-50, 1:1000); goat anti-DCX (Santa-Cruz sc-8066, 1:100); rat anti-BrdU (Abd Serotec MCA2060, 1:300); rabbit anti-GFAP (Agilent Z033401-2, 1:1000); rabbit anti-Calretinin (Swant 7699/3H, 1:2000); mouse anti-Nestin (Merck-Millipore MAB353, 1:1000); mouse anti-Gad67 (Merck-Millipore MAB5406, 1:200); rabbit anti-Parvalbumin (Abcam ab11427, 1:2000); rabbit anti-CB1 (Abcam ab23703, 1:100); rabbit anti-RFP (Abcam ab62341, 1:500); goat anti-Sox2 (Santa Cruz sc-17320, 1:100); rabbit anti-CCK (Biozol LS-C414751-100, 1:50); chicken anti-Parvalbumin (SYSY 195006, 1:250); mouse anti-GFP (Thermo Fisher A-11122, 1:1000); and rabbit anti-Calbindin (Swant CB38, 1:2000). The secondary Alexa Fluor-conjugated antibodies from Life Technologies were diluted 1:1000 in PBS. All slices were stained with a diaminodiphenylindole solution 0.2 µg/ml in PBS for 30 min and mounted using Mowiol 4-88 reagent from Carl Roth. For details regarding the quantification, see Supplementary Methods and Supplementary Figure 1.

In Situ Hybridization

In situ hybridization (ISH) for layer-specific markers was performed as described previously (Wagener et al. 2016). In brief, ISH for neuron-derived neurotrophic factor (Ndnf; also known as A930038C07Rik), Rgs8, Rorb (also known as Ror beta), Etv1 (also known as Er81), as well as TC1460681 (TC) were performed with digoxigenin (DIG)-labeled cRNA probes. They were generated from the appropriate plasmids containing full-length cDNA inserts specific for the respective laminar marker for Ndnf, Rgs8, Rorb, and Etv1 (Source BioScience order

numbers: “Ndnf,” IRAPv968E1091D; Rgs8, IRAPv968E09162D; Rorb, IRAPv968D1267D; and Etv1, IRAKp961E106Q). TC1460681 was amplified from genomic cDNA with the appropriate primers (forward: TCCTCAGAGAGTCAGTCCTTCC, reverse: TACTGTGATCGGTTTTGGAGTG; Boyle et al. 2011), and cloned into the pCR-BluntII-TOPO Vector (Invitrogen), transfected into JM 109 competent *Escherichia coli* (Promega), amplified in overnight cultures, and purified with a purification kit (Qiagen). All plasmids underwent restriction digestion with appropriate enzymes. In vitro transcription was performed using a DIG RNA labeling kit (Roche). The sizes of the full-length probes were reduced to approximately 350 base pairs via alkaline hydrolysis with 0.2 M sodium carbonate and 0.2 M sodium bicarbonate at pH 10.2.

Animals for ISH were perfused transcardially with 10 ml of 10% sucrose, followed by 200 ml of 4% paraformaldehyde in 0.1 M phosphate buffer (PB), pH 7.4. Brains were dissected out of the skull and postfixed for 2 h in 4% paraformaldehyde, then cryoprotected in 20% sucrose in PBS overnight at 4°C. The brains were immersed in isopentane and snap frozen at –20°C. The frozen brains were recovered from the isopentane and stored at –80°C. Coronal sectioning was done with a cryostat (CM 3050S; Leica) at 40 µm thickness. The sections were collected free floating in PBS (dissolved in diethyl pyrocarbonate (DEPC)-treated H₂O) and were rinsed three times in 2× standard saline citrate (SSC - 1× SSC = 0.15 M NaCl, 0.015 M sodium citrate, pH 7.0). They were pretreated for 15 min in hybridization buffer (HB; 50% formamide, 4× SSC, 250 µg/ml denatured salmon sperm DNA, 100 µg/ml tRNA, 5% dextran sulfate, and 1% Denhardt's solution) diluted 1:1 in 2× SSC at room temperature, followed by 1 h of incubation in pure HB at 55°C. Probe hybridization with DIG-labeled probes (200 ng/ml) was carried out overnight at the same temperature. Posthybridization stringency washes were performed with 2× SSC (2× 15 min, at room temperature), 2× SSC/50% formamide (15 min, at 65°C), 0.1× SSC/50% formamide (15 min, at 65°C), 0.1× SSC (2× 15 min, at 65°C) and 0.01 M TBS, pH 7.4 (2× 10 min, at room temperature). The probes were detected by anti-DIG Fab fragments conjugated to alkaline phosphatase (raised in sheep; Roche) diluted 1:1500 in TBS-containing blocking agent (Roche, at 4°C overnight). Hybridized probes were stained with nitroblue tetrazolium and 5-bromo-4-chloro-3-indolylphosphate (Roche). Development of the staining reaction was monitored with a stereo microscope. After the desired intensity was achieved, sections were rinsed again in TBS and mounted in Kaiser's glycerol gelatin (Merck).

Imaging

With the exception of Figure 5, imaging was performed using the confocal laser scanning microscope Olympus FV1000, equipped with Olympus objectives UPlanS Apo ×60 (numerical aperture (NA) 1.35 oil) or UPlanS Apo ×20 (NA 0.85 oil) and FLUOVIEW 4.2.1.20 software.

Imaging of brightfield images (Fig. 5) was performed with an Axio Imager M2 (Zeiss) controlled by a Neurolucida system (Version 11; BF Bioscience). The images were acquired as virtual tissues (consisting of 3–5 z-planes in 5 µm steps) and are presented as minimum intensity projections (MIP). The MIPs were taken from five consecutive coronal brain sections, each including a chromogenic ISH for an individual laminar marker. In order to merge the 5 MIPs, each section was assigned to a different false color and they were merged using Adobe Photoshop.

Western Blotting

All Western blots (WBs) were performed with the WB-system BIORAD Mini-PROTEAN Tetra System. The protocol was adapted from Trotter (Trotter et al. 2014). In brief, the tissue was homogenized in M-PER and HALT (Thermo Fisher), supplemented with 3× Laemmli buffer and incubated at 95 °C for 10 min. To obtain dentate gyrus samples, freshly dissected hippocampi were cut into 500 μm sections using a McIlwan tissue chopper and the dentate gyrus was subsequently excised from five slices. Acrylamide gels with 8% and 15% running gels stacked on each other were used to separate Reelin and Actin on the same gel. The membrane was cut at the level of the 100 kDa marker band, blocked with 5% milk powder in tris-buffered saline with 0.1% Tween20 (TBST20) for 1 h at RT before incubation with mouse anti-Reelin antibody (Merck Millipore MAB5364) and rabbit anti-Actin antibody (Sigma-Aldrich A-2066), each diluted 1:1000 in 5% milk powder in TBST20 overnight. Horseradish peroxidase-conjugated antibodies from Abcam were used as secondary antibodies and the signals were detected with SuperSignal WestPico Chemiluminescent Substrate Kit (Fisher Scientific). Signal intensity was analyzed using the Fiji package of the ImageJ software (Schindelin et al. 2012; Schneider et al. 2012).

Behavioral Experiments

Animals

A cohort of male, naïve mice with the following genotypes were used: *Reln^{fl/fl} Dlx5/6-Cre* positive, *Reln^{fl/fl} Dlx5/6-Cre* negative, and *Reln^{wt/wt} Dlx5/6-Cre* positive. The mice were housed with an inverted 12 h–12 h light–dark cycle (lights on from 7 pm to 7 am), and all behavioral testing was carried out during the dark phase of the cycle. In all experiments, the trials were recorded using the Ethovision tracking system (Version XT 8.5, Noldus Technology).

Elevated Plus Maze Test

The apparatus was constructed from white waterproof polyvinyl (PVC) foam material and consisted of four interconnected arms (30 cm long × 5 cm wide) radiating from a 5 cm² central square. This was elevated 70 cm above the floor on a metallic stand. One pair of opposing arms was surrounded by walls 15 cm high (closed arms), whilst the remaining two arms were exposed and contained a 2-mm high border along the outer edges of the arms (open arms). The maze was illuminated by two dimmable floor uplighters that provided light intensity of 70–75 lux in the open arms. A trial commenced by gently placing the mouse in the central square facing one of the open arms and allowed it to explore freely for 5 min. Analysis of automated measures included the distance moved over 5 min, the time spent in the open arms and frequency of entrance into the open arms.

Open Field Spontaneous Locomotor Activity

The experimental setup consisted of four identical arenas (length × width × height: 50 cm × 50 cm × 50 cm) made of white waterproof PVC foam material. Each arena was virtually divided into a center zone (15 cm × 15 cm), middle zone (30 cm × 30 cm), and an outer zone (45 cm × 45 cm). Four individually dimmable lamps positioned above the apparatus provided even illumination in each arena (50 lux). Each mouse was introduced into the arena facing the wall and allowed to explore freely for 40 min. Locomotor activity was indexed as the distance moved in 5 min consecutive time bins. Additionally, the percentage of

time spent in the central zone of the arena was calculated as an index for anxiety-related behavior.

Morris Water Maze Spatial Reference Memory

The Morris water maze (MWM) test involved 10 *Reln^{fl/fl} Dlx5/6-Cre* positive, 9 *Reln^{fl/fl} Dlx5/6-Cre* negative, and 10 *Reln^{wt/wt} Dlx5/6-Cre* positive male mice. Spatial reference memory was assessed in a white plastic circular tank (150 cm in diameter by 75 cm in height), under mild lighting conditions (80 lux as measured at the maze center). Four arbitrary cardinal points (N, E, S, and W) were equally spaced along the circumference of the pool, which was then conceptually divided into four equal quadrants designated as NE, SE, SW, and NW. The maze was positioned in a room enriched with unique proximal and distal extra-maze cues to aid spatial navigation. The mice were first trained for 2 days, with four consecutive trials (8 min intertrial interval (ITI)) per day, using the nonspatial visible platform procedure. The pool was surrounded by curtains to occlude extra-maze cues, while the submerged platform was marked by a prominent cue. The release point and platform location varied across trials. A trial ended when the mouse escaped onto the platform, or after 60 s had elapsed, at which point the mouse was guided to the platform by the experimenter. All mice were allowed to remain on the platform for 15 s before being taken out. Thereafter, spatial reference memory acquisition was conducted over 10 days (four trials per mouse per day; 8 min ITI). Mice were trained to utilize the presence of extra-maze cues, in order to navigate and escape onto a platform submerged 1 cm below the water surface. A trial ended when the mouse climbed onto the platform, or after 60 s had elapsed, during which it was gently guided by the experimenter to the platform. The mice were allowed to remain on the hidden platform for 15 s before being removed from the pool. Spatial learning was inferred by computing latency to the hidden platform as the main dependent variable.

Following successful acquisition with the criterion that latency to find the platform across four consecutive trials was 20 s or less, a 90 s probe test was conducted at 24 h, 7 days, and 28 days after the last acquisition trial, in order to examine long-term spatial reference memory retention. Here, the platform was removed from the pool and the mice gently released from a new location directly opposite from the target quadrant. Search preference for the correct spatial location was measured as the proportion of time spent in the target quadrant.

Statistics

Statistical analyses were performed using the SPSS Statistics for Windows program (IBM Corp. Version 22.0: IBM Corp.). Non-behavioral data were analyzed using one-sample t-test (Fig. 1D) and comparisons of means for two independent groups using the Student's t-test (t-test). Behavioral data were first analyzed for assumption of normality using the “Shapiro-Wilk's W” statistic and homogeneity of variances using Levene's test. One-way analysis of variance (ANOVA) was used for comparisons of means for the three independent genotype groups. Data derived from repeated testing were subjected to a mixed-design ANOVA with the inclusion of time-bins, delay, or days as within-subject factors and genotype as between-subjects factor. Sphericity was evaluated with Mauchly's test of sphericity. When violated, the degrees of freedom were corrected using Greenhouse-Geisser estimates of sphericity. Significance was set at $P < 0.05$

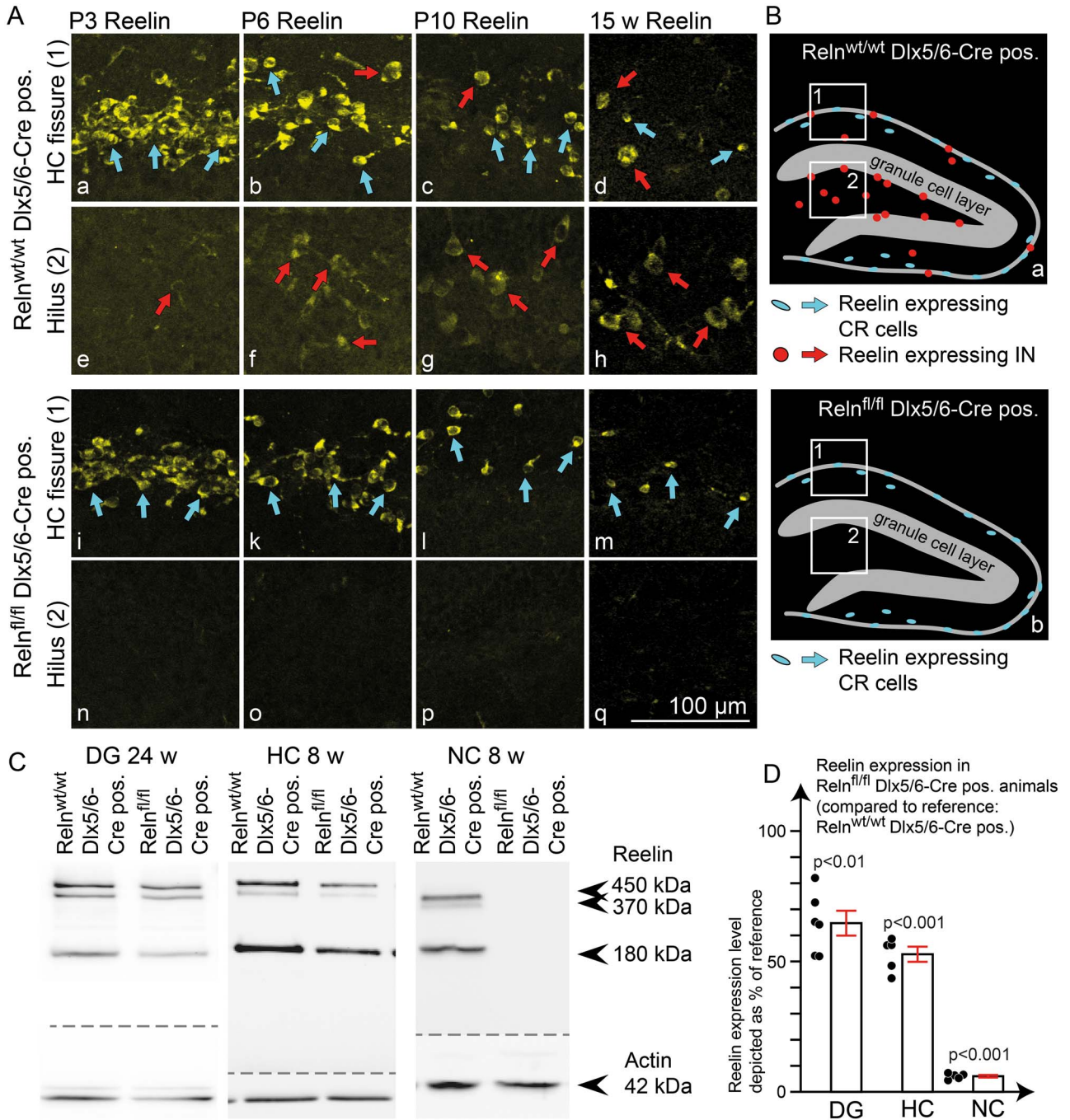


Figure 1. Reelin expression pattern in IN-specific Reelin knockout mice. (A) Immunohistochemical staining for Reelin at different developmental stages (age: P3, P6, P10, and 15 weeks) in IN-specific Reelin knockout mice (Rein^{fl/fl} Dlx5/6-Cre positive) compared with controls (Rein^{wt/wt} Dlx5/6-Cre positive). Stainings confirmed normal Reelin expression in CR cells (detail from the hippocampal fissure in control (a–d) and IN-specific Reelin knockout animals (i–m)) and a complete lack of Reelin expression in INs (detail from the hilus in control (e–h) and IN-specific knockout animals (n–q)). (B) Schematic drawing of Reelin-expressing cells in the dentate gyrus in control (a) and IN-specific knockout animals (b). (C) WB analysis from adult mouse brains (age: 24 weeks for DG; age: 8 weeks for NC and HC) revealed a profound reduction of Reelin expression in the dentate gyrus and total HC and a near-complete loss of Reelin in the NC. (D) WB quantifications showed a Reelin reduction of 94 ± 0.5% in the NC, 47 ± 3% in the HC (one-sample t-test against 100% control; N = 5 animals; age: 8 weeks), and 35 ± 5% in the dentate gyrus (one-sample t-test against 100% control; N = 6 DG samples (equally sampled from three animals); age: 24 weeks). All values were normalized to actin and depicted as a percentage of reference (Rein^{wt/wt} Dlx5/6-Cre pos.). The results were depicted as mean ± SEM. Dots represent single values for each animal for NC and HC. In the case of the DG, dots represent measurements for left and right DG from three animals per genotype.

(two-tailed), or according to Bonferroni adjusted significance for levels of multiple comparisons. Data are presented as means \pm standard error of mean (SEM). *P*-values in the figures are based on the corresponding test detailed in the figure legend.

Results

Interneuron-Specific Knockout of Reelin

During embryonic development of the NC and HC Reelin originates exclusively from CR cells (Ogawa et al. 1995), while perinatally inhibitory INs also start to become an important source of Reelin (Alcantara et al. 1998; Pesold et al. 1998). To investigate the specific function of Reelin from inhibitory INs, we crossbred a mouse line with loxP sites flanking the first exon of the *reelin* gene (Lane-Donovan et al. 2015) with an IN-specific *Dlx5/6*-Cre line (Monory et al. 2006). The *Dlx5/6* promoter is specifically active in INs during their early development within the ganglionic eminence (Boncinelli 1994; Simeone et al. 1994; Hevner et al. 2003; Ruest et al. 2003; Monory et al. 2006). Reelin-expressing INs belong to different subtypes of INs (Pesold et al. 1999; Pohlkamp et al. 2014; Tasic et al. 2018), emerging from both the medial and caudal ganglionic eminence (Miyoshi et al. 2010). To confirm the activity of Cre recombinase in all Reelin-expressing INs in the *Dlx5/6*-Cre line, we applied a tdRFP reporter line (Luche et al. 2007) to visualize cells, which had undergone Cre-dependent DNA recombination. Double-immunohistochemical stainings for this reporter and Reelin confirmed that all Reelin-expressing INs in the HC and NC of *Dlx5/6*-Cre mice exhibited Cre-dependent DNA recombination, while CR cells were not affected (Supplementary Fig. 2). *Dlx5/6*-Cre recombinase is already expressed in INs at embryonic stages. The *Dlx5/6* Promoter is active commencing from E9.5 in mice (Simeone et al. 1994). This results in Cre-dependent inactivation of the *reelin* gene in INs several days before the onset of Reelin expression between P0 and P5 in these cells (Alcantara et al. 1998; Pesold et al. 1998). Immunohistochemical staining for Reelin in *Reln^{fl/fl} Dlx5/6*-Cre positive mice confirmed the lack of Reelin protein expression in INs as early as postnatal day 3 (P3) (Fig. 1A n), corresponding with the time point of expression onset in inhibitory INs in control mice (Fig. 1A e; red arrow). With increasing age, differences became more pronounced due to the increase in Reelin expression in inhibitory INs in control animals (Fig. 1A f–h, red arrows compared with Fig. 1A o–q). In contrast, Reelin expression in CR cells was unaltered in the IN-specific Reelin knockout mouse throughout development (Fig. 1A a–d, blue arrows compared with Fig. 1A i–m). Other sources of Reelin, such as mitral cells in the olfactory bulb or layer II cells in the entorhinal cortex, were also unaffected (data not shown). Quantitative WB analysis revealed a $35 \pm 5\%$ reduction of Reelin expression in the dentate gyrus, $47 \pm 3\%$ in the HC and $94 \pm 0.5\%$ reduction in the NC of adult IN-specific Reelin knockout mice (Fig. 1C, D). These results suggest that the contribution of INs to Reelin expression differs among brain areas. Taken together, these data confirm Reelin expression to be exclusively depleted in INs in the IN-specific Reelin knockout mouse, but not in other cell types, including CR cells.

Reelin Expression Pattern in the Dentate Gyrus

While Reelin expression is well documented in the adult NC by recent studies (Pohlkamp et al. 2014), much less is known regarding the distribution of Reelin-expressing cells in the adult dentate gyrus. To further examine Reelin protein expression in

the adult dentate gyrus, we quantified the number of Reelin-expressing INs and CR cells within different compartments of the dentate gyrus (Fig. 2). The compartmentalization was done as follows: an area of 60 μ m above and below the hippocampal fissure was defined as ‘fissure’ (in this area, all CR cells are included). The SGZ, in which IN density is especially high and adult neurogenesis takes place, was defined as 10 μ m above and below the border between the granule cell layer and hilus. Additional compartments were the hilus (defined by the borders of the granule cell layer), the iML (defined as the area between the granule cell layer and the area already defined as ‘fissure’) and the CA1 region next to the fissure (stratum lacunosum moleculare (LM) and radiatum (rad)), to include both areas surrounding the CR cell-containing fissure. Due to the extension of the area defined as ‘fissure’ over 60 μ m into the ML, the area defined as ‘fissure’ already included the outer ML. To distinguish both Reelin-expressing CR cells and Reelin-expressing IN, we used tdRFP-reporter mice to label the inhibitory INs. We found 35–61% of all INs to be Reelin-immunoreactive (Fig. 2A,B), with clear regional differences. The proportion of INs expressing Reelin turned out to be higher next to the hippocampal fissure (Fis) and within the ML (iML) (61% Fis; 57% iML) compared with the stratum LM/rad, the SGZ and the hilus (35% LM/rad; 36% SGZ; and 36% Hilus) (Fig. 2B). Quantification of Reelin-expressing CR cells, identified as ‘small’ tdRFP-negative cells within a distance of 60 μ m around the fissure, confirmed their high abundance in the adult dentate gyrus. Notably, the number of Reelin-expressing CR cells was significantly increased in IN-specific knockouts, resulting in an overall unchanged number of Reelin-expressing cells around the hippocampal fissure.

Evaluation of Possible Autocrine Effects of Reelin

It has been a matter of debate whether Reelin acts exclusively in a paracrine way, or whether it may also mediate autocrine functions (Derer 1985; Coulin et al. 2001). Since INs are malpositioned in *reeler* mutant mice (Hevner et al. 2004), we addressed whether Reelin depletion in INs might affect INs themselves. Analysis of the tdRFP reporter did not reveal any changes in total IN densities in the dentate gyrus (Fig. 2B) and in the NC (Fig. 3A). However, the distribution of INs subgroups might be altered. For instance, in heterozygous *reeler* mice a decrease in glutamate-decarboxylase *Gad67*-expressing INs, as well as in Parvalbumin-expressing INs, has been reported (Nullmeier et al. 2011). Of note: while *Gad67* is detected in virtually all INs in ISH, this is not the case with immunohistochemical stainings, possibly due to different localization of the protein within the cells (Houser 2007). Thus, we used immunohistochemical staining for *Gad67*, the calcium-binding proteins Parvalbumin, Calbindin-28 kDa, Calretinin and the Cannabinoid receptor 1 (CB1), to label distinct subpopulations of INs in the NC and dentate hilus.

We identified an increase in CB1 and Calretinin staining intensity within the iML (Fig. 3C, D) and observed increased numbers of Calretinin-positive cells in the hilus (Fig. 3B). However, double labeling with the IN-specific tdRFP reporter revealed that the hilar cells, as characterized by enhanced Calretinin expression, are not inhibitory IN, but may rather represent hilar mossy cells (Fig. 3B'). As mossy cells project to the iML, this may also account for the higher Calretinin immunoreactivity in this area (Fig. 3C). Other IN markers revealed no obvious changes across genotypes regarding the number of positive cells in NC and dentate hilus (Fig. 3B and Supplementary Fig. 3).

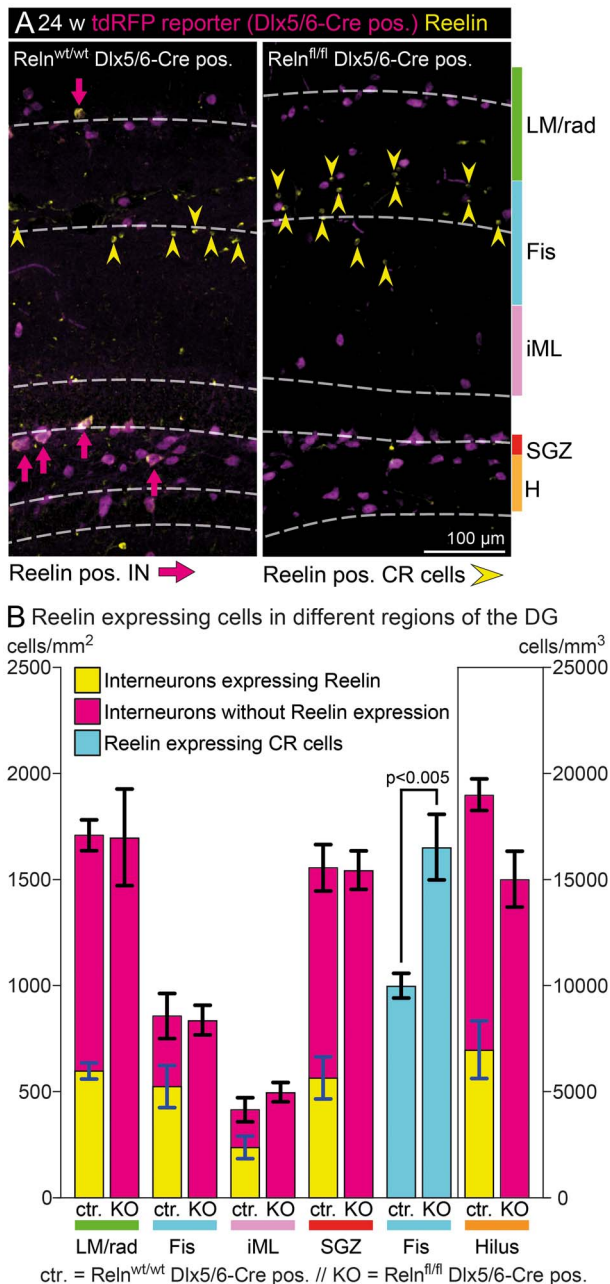


Figure 2. Reelin expression pattern in the mature dentate gyrus. (A) Immunohistochemical staining for tdRFP and Reelin was used to analyze the total number of INs, the number of Reelin-expressing INs and Reelin-expressing CR cells in different areas of the dentate gyrus. INs were identified by tdRFP reporter staining, while CR cells were identified as small Reelin-expressing cells without tdRFP expression. (B) Quantification of cell numbers in different layers. The total number of INs and their distribution within the dentate gyrus was unchanged in IN-specific Reelin knockout mice. In addition, as expected, all INs proved to be Reelin-negative in this model. Interestingly, the number of Reelin-expressing CR cells was significantly increased in adult IN-specific Reelin knockout mice (*t*-test; *N* = 5; age: 24–30 weeks; error: ±SEM), and the number of additional CR cells (654 ± 108) corresponded well to the number of INs that lost Reelin expression within a distance of 60 μm around the fissure (Fis) (524 ± 99). Abbreviations: LM/rad—Stratum lacunosum-moleculare and parts of stratum radiatum; Fis, fissure (±60 μm around the hippocampal fissure); iML, inner molecular layer; SGZ, subgranular zone (±10 μm around the inner border of the granule cell layer); and H, hilus.

Reelin Expressed by Interneurons is Neither Required to Establish Nor to Maintain Cortical Layers

The development of neuronal layers, in particular in the dentate gyrus, is not yet completed when perinatal Reelin expression in INs is initiated. So far, it is unknown whether Reelin from INs contributes to the formation of the granule cell layer. Furthermore, in the adult dentate gyrus, granule cell dispersion in TLE has been linked to a loss of Reelin-expressing INs (Haas et al. 2002; Chai et al. 2014). Thus, Reelin has also been proposed to play a role in the maintenance of the established structures throughout life (Frotscher et al. 2009). To examine whether Reelin from INs plays a role in the establishment or in the maintenance of neuronal layers, we investigated neuronal layering in the dentate gyrus and NC of adult IN-specific Reelin knockout mice.

Quantitative analysis of granule cell layer thickness and the number of NeuN-positive neurons in the ML of IN-specific Reelin knockout mice (15 weeks) did not reveal any differences compared with wild-type mice (Fig. 4A–C). To take a closer look at granule cell morphology, we also applied breeding with a Thy1eGFP mouse line (Feng et al. 2000), which expresses the green fluorescent protein in a subset of neurons (Fig. 4D). Representative images of reconstructed Thy1eGFP-positive granule cells are shown in Fig. 4E. Measurements of the length, width, and branching angle of single dendrites (branching order 1–4) were performed using Imaris (branching order 1–4 have been included in the analysis, as branching order up to four was regularly found in nearly all reconstructed cells—in rare cases branching order up to seven was found in granule cells in both knockout and control animals). The analysis revealed unchanged morphology of granule cell dendrites in IN-specific Reelin knockout mice (Fig. 4F–H).

Laminar organization in the NC was evaluated by ISH, detecting layer-specific mRNAs (Boyle et al. 2011; Wagener et al. 2016). The mRNA for *Ndnf*, also known as RIKEN cDNA A930038C07 gene, has been used to label cells in layer I, mRNA for Regulator of G-protein signaling 8 (*Rgs8*) for layer II/III, mRNA for RAR-related orphan receptor B (*Rorb*) for layer IV, mRNA for ETS variant gene 1 (*Etv1*) for layer Va and mRNA for immunoglobulin heavy chain TC1460681 (*TC*) to label layer VI. The depth of the NC was equally divided into 20 bins and the signal intensity for every marker was quantified for every bin (for details of quantification, see Supplementary Fig. 4). The quantification revealed an intact layering of the NC, which was indistinguishable from the control animals (Fig. 5).

In summary, Reelin from INs does not appear to play a major role in the establishment or maintenance of neuronal layers in the NC and dentate gyrus.

Normal Learning and Memory Function in IN-Specific Reelin Knockout Mice

Reelin has been shown to play a role in different aspects of synaptic plasticity, such as dendritic spine development (Liu et al. 2001; Niu et al. 2008; Leemhuis et al. 2010; Bosch et al. 2016), modulation of NMDA-receptor transmission and composition (Chen et al. 2005; Groc et al. 2007; Campo et al. 2009), vesicle release (Hellwig et al. 2011; Bal et al. 2013), and LTP (Weeber et al. 2002; Beffert et al. 2005). In addition, behavioral deficits were shown in heterozygous *reeler* mice (Tueting et al. 1999; Rogers et al. 2013), while others have reported mild or inconsistent findings (Podhorna and Didriksen 2004; Krueger et al. 2006). Here,

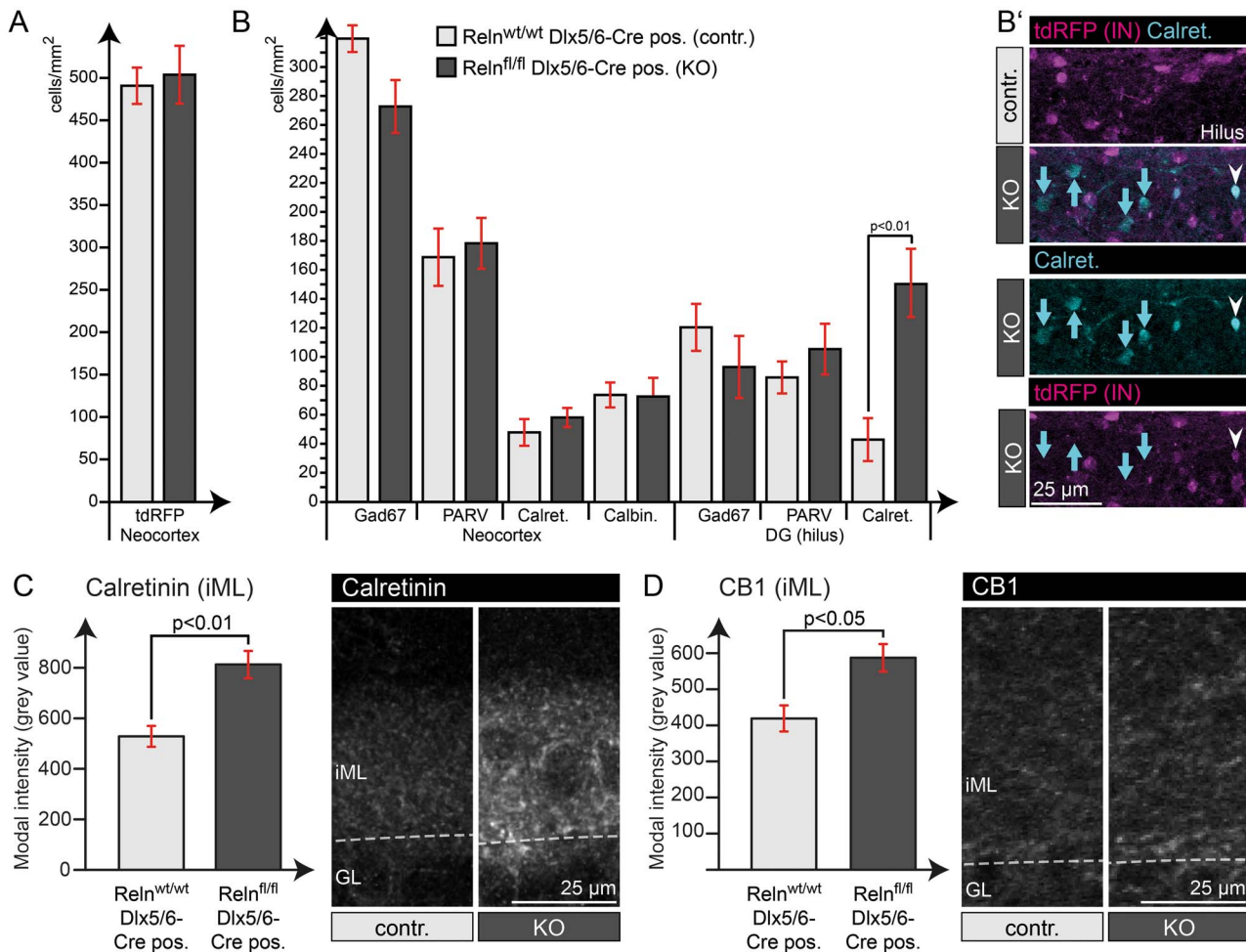


Figure 3. Quantification of IN markers revealed higher Calretinin expression in the hilus. (A) Quantification of tdrRFP-positive INs in the NC showed normal total IN numbers in IN-specific Reelin knockout mice. (B) Quantification of cells expressing different IN marker proteins throughout the NC and dentate gyrus revealed an unaltered IN composition within these areas. The significant increase in Calretinin-expressing cells in the dentate gyrus could be assigned to an increase in Calretinin expression in tdrRFP-negative hilar mossy cells (B' – blue arrows), while tdrRFP-positive INs were not affected (white arrowheads). (C) Quantification of Calretinin intensity in the iML, the area of the mossy cell projections, confirmed this significant increase in Calretinin expression. (D) In addition, quantification of CB1 intensity within the iML also revealed a slight increase in expression (t-test; $N = 5$ animals; age: 24–30 weeks; error: \pm SEM).

we examined the extent to which IN-derived Reelin modulates behavioral function by testing for cognitive and noncognitive processes known to depend on the HC (O'Keefe and Nadel 1978; Bannerman et al. 2014; Zhang et al. 2014). Assessment in the open field (OF) paradigm revealed intact locomotor habituation in IN-specific Reelin knockout mice. Despite overall increased activity in Cre-positive Rein^{wt/wt} mice, activity levels did not differ between IN-specific Reelin knockout mice and the Cre-negative Rein^{fl/fl} control group (Fig. 6A), indicating that differences in activity levels are unlikely to stem from lack of Reelin. Anxiety-related behavior was unaltered, as evidenced by the comparable time spent in the center of the OF arena (Fig. 6B) and open arms of the elevated plus-maze (Fig. 6C) across all genotypes. Similarly, the acquisition (Fig. 6D) and time-dependent long-term retention of spatial reference memory (Fig. 6E) was comparable for all genotype groups. Thus, the lack of Reelin from INs in the adult brain has minimal impact in vivo, as evidenced by largely normal behavioral function and intact ability in spatial learning and memory.

Reelin From Interneurons and Adult Neurogenesis in the Dentate Gyrus

Previous work has shown that adult neurogenesis is severely decreased in the *reeler* dentate gyrus (Won et al. 2006; Zhao et al. 2007; Sibbe et al. 2015). We thus aimed to determine whether IN-derived Reelin plays a role in the regulation of adult neurogenesis. Unlike the classical *reeler* mouse, the morphology of the stem cell niche was unaffected in the IN-specific Reelin knockout mouse (Supplementary Fig. 5). This is important as the morphological alteration of the stem cell niche as such might also account for changes in adult neurogenesis (Stolp and Molnar 2015). To investigate the exact position and morphological integration of Reelin-expressing INs within the adult stem cell niche, we used POMCeGFP mice (Overstreet et al. 2004) to visualize immature granule cells in the adult stem cell niche. Immunohistochemical stainings revealed that the cell bodies of Reelin-expressing INs were located within the SGZ. They were in close contact with eGFP-positive immature granule cells,

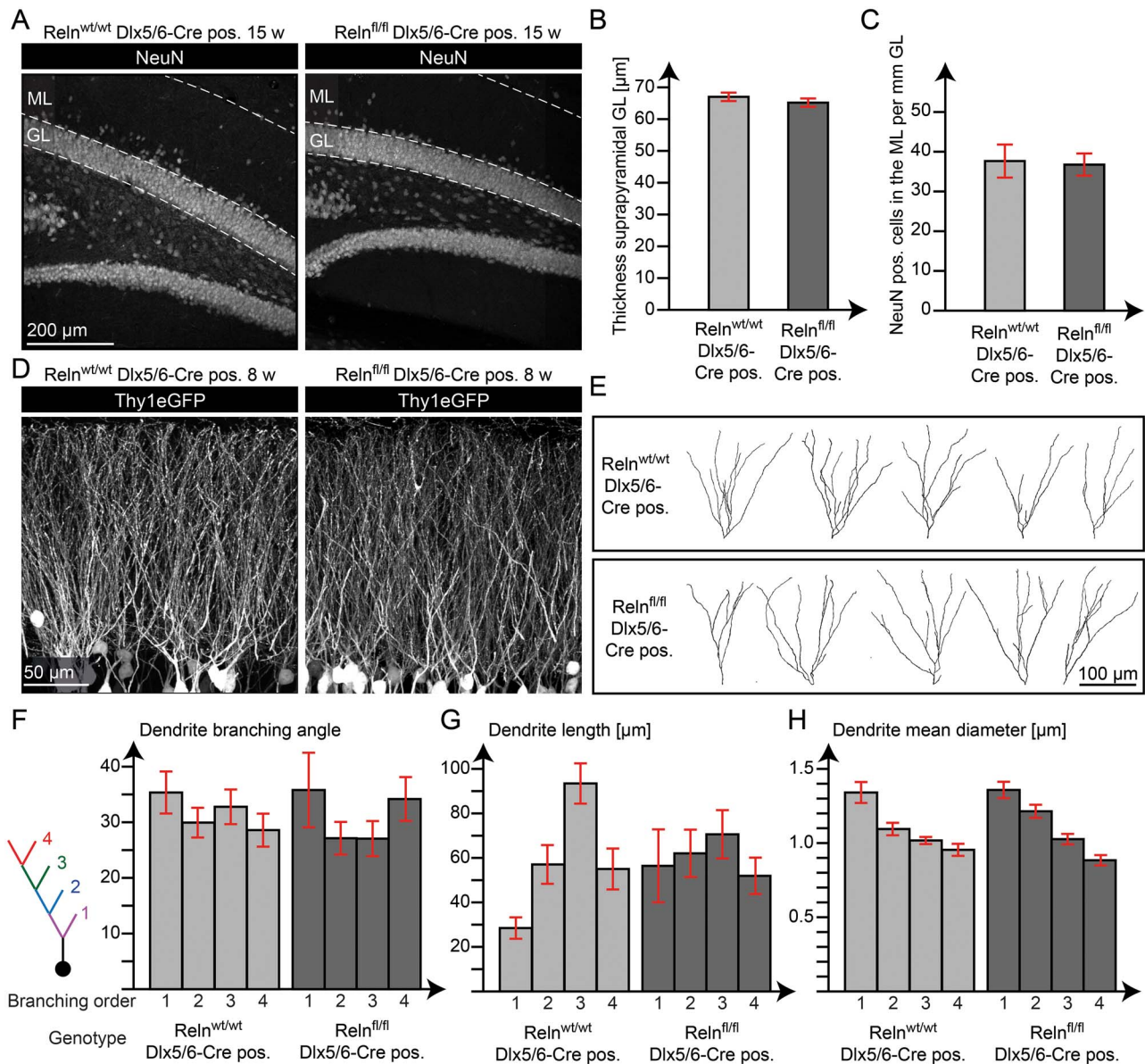


Figure 4. Reelin from INs did not affect maintenance of the granule cell layer. (A) Immunohistochemical staining for NeuN in the dentate gyrus of adult animals (15 weeks). Quantification of the thickness of the suprapyramidal granule cell layer (GL) (B) and the number of NeuN-positive cells in the suprapyramidal ML (C) showed no significant difference (t-test; $N = 5$ animals; age: 15 weeks; error: \pm SEM). (D) The Thy1eGFP mouse line (Feng et al. 2000) was used to reveal the morphology of granule cells. (E) Reconstruction of single granule cell dendrites. The branching angle (F), length (G), and mean diameter (H) were evaluated for single dendrites at different branch order (1–4). The quantifications revealed no significant difference in granule cell dendrite morphology (t-test; $N = 18$ –44 dendrites sampled from five animals per group; age: 8 weeks; error: \pm SEM).

doublecortin-labeled immature granule cells and radial glia-like cells (RGLCs) both in young animals, when INs have just started to express Reelin (P6 – Fig. 7A a,a'), and also in adult animals (24 weeks – Fig. 7A b–e). We identified these Reelin-expressing INs within the stem cell niche as Cholecystinin (CCK)-positive hilar commissural associational path (HICAP) cells (Freund and Buzsaki 1996), while none of the Parvalbumin-positive basket cells expressed Reelin (Fig. 7B a–b). The schematic 3D drawing in Figure 7C illustrates the regular distribution pattern of these two types of INs within the stem cell niche and the close contact of immature granule cells to Reelin-expressing INs. The general composition of the stem cell niche in this schematic drawing is

based on recently reviewed data (Fuentealba et al. 2012; Kempermann et al. 2015).

To address a potential effect of Reelin ablation from INs, we quantified cell proliferation and the number of immature neurons in the adult dentate gyrus. A single BrdU injection in 12-week-old animals and quantification of BrdU- and Doublecortin-positive immature granule cells (Francis et al. 1999) two weeks later revealed a slight effect on adult neurogenesis (Fig. 8B–D) which, however, is much less pronounced when compared with the effects in the classical *reeler* mouse (Won et al. 2006; Zhao et al. 2007; Sibbe et al. 2015). We substantiated this weak effect using additional experimental designs: we therefore included

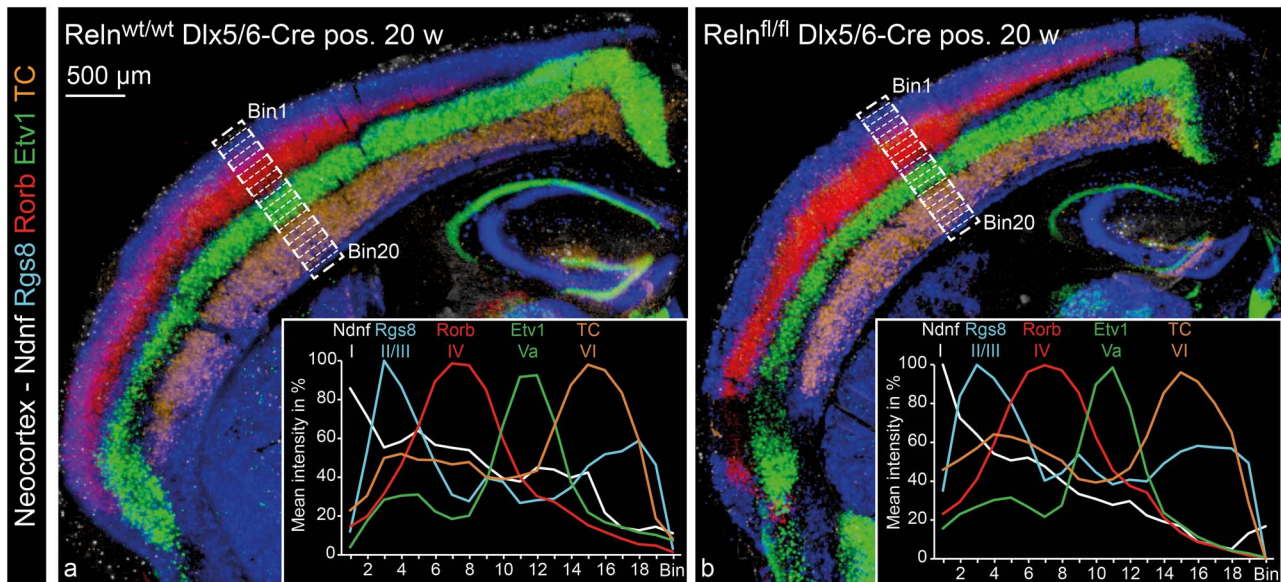


Figure 5. Neocortical layering in IN-specific Reelin knockout mice. ISH for five different probes labeling specific layers of the NC was performed on consecutive cryosections from controls (a) and IN-specific Reelin knockout mice (b). Probes used were *Ndnf* for layer I, *Rgs8* for layer II/III, *Rorb* for layer IV, *Etv1* for layer Va and TC for layer VI. The consecutive sections are represented as a merger of five individually colored micrographs. Each of the five micrographs is a MIP of four optical planes (z-distance 4 μ m). For quantification, the depth of the NC had been equally subdivided into 20 bins (starting with bin 1 at the pial surface and ending with bin 20 at the ventricular zone). Mean staining intensity was evaluated for each bin and depicted as a percentage ranging from maximum staining intensity (100%) to minimum staining intensity (0%) for each analyzed image. Diagrams show mean values for six analyzed images, equally sampled from three animals for both genotypes (Supplementary Fig. 4 includes the individual data sets).

continuous application of BrdU via the drinking water for two weeks, to increase the total number of BrdU-labeled cells (Fig. 8E). We also included quantification of Ki-67, a marker of proliferating cells (Kee et al. 2002) (Fig. 8E). Although additional quantitative evaluations failed to yield significant differences, in all five independent experiments (based on 18 animals per genotype in total), a trend toward a decrease in neurogenesis of about 10% was detected in conditional knockout mice (Fig. 8C–E). From these findings, we conclude that the lack of Reelin expression in INs exerts a weak but consistent effect on adult neurogenesis within an otherwise intact stem cell niche. In addition, DCX-positive immature neurons exhibited normal orientation and dendritic arborization in IN-specific Reelin knockout mice (Fig. 8F).

Complexity of GFAP Filaments is Reduced in Dentate Gyrus Astrocytes

Since RGLCs are also severely affected during development in the *reeler* dentate gyrus (Weiss et al. 2003; Brunne et al. 2013), we studied the morphology of Nestin- and GFAP-positive intermediate filaments in these RGLCs, which are still present in the mature dentate gyrus and serve as stem cells for adult neurogenesis (Seri et al. 2001; Steiner et al. 2004). Nestin- and GFAP-positive processes of RGLCs, identified by their prominent radial process spanning through the granule cell layer, were unaffected (Fig. 9A). In addition, we examined GFAP in astrocytes, as it was shown that GFAP-positive astrocytes may respond to Reelin (Förster et al. 2002; Frotscher et al. 2003; Brunkhorst et al. 2015). In immunohistochemical stainings, the overall density of GFAP filaments appeared to be decreased in the ML and in the hilus of the dentate gyrus (Fig. 9B). Sholl analysis of GFAP-positive astrocytes in the ML confirmed this impression, showing slightly

reduced filament complexity (Fig. 9B). In addition, quantitative analysis revealed a significant reduction of the total volume of GFAP filaments in the dentate gyrus in IN-specific Reelin knockout mice (Fig. 9C). Thus, while RGLCs are unaffected, astrocytes show a reduction in GFAP filament complexity in IN-specific Reelin knockout mice, leading to a significant reduction in total GFAP filament volume.

Effects in Interneuron-Specific Reelin Knockout Mice Were Not Due to a General Reduction in Reelin Protein Expression, As Shown by Analysis of Mice With Heterozygous Reelin Deletion

IN-specific Reelin knockout mice exhibited a Reelin reduction of $47 \pm 3\%$ in the HC, similar to heterozygous *reeler* animals. To examine whether a reduction of Reelin by approximately 50% causes a similar phenotype, we also tested for the presence of differences (as found in IN-specific Reelin knockout mice) in heterozygous Reelin knockout mice (*Reln*^{wt/dl}) and compared them with wild-type animals (*Reln*^{wt/wt}).

Interestingly, all differences found in IN-specific Reelin knockout mice are absent in heterozygous Reelin knockout mice. Calretinin and CB1 expression in the iML were highly comparable between heterozygous Reelin knockout and wild-type animals (Fig. 10A,B). Regarding CR cell numbers around the hippocampal fissure (Fig. 10C) and GFAP filaments in the dentate gyrus (Fig. 10D), we also found no significant difference between the genotype groups. Overall, these experiments confirmed that the effects observed in IN-specific Reelin knockout mice were not attributed to a general decrease in Reelin protein expression, but were a consequence of the specific loss of Reelin in INs.

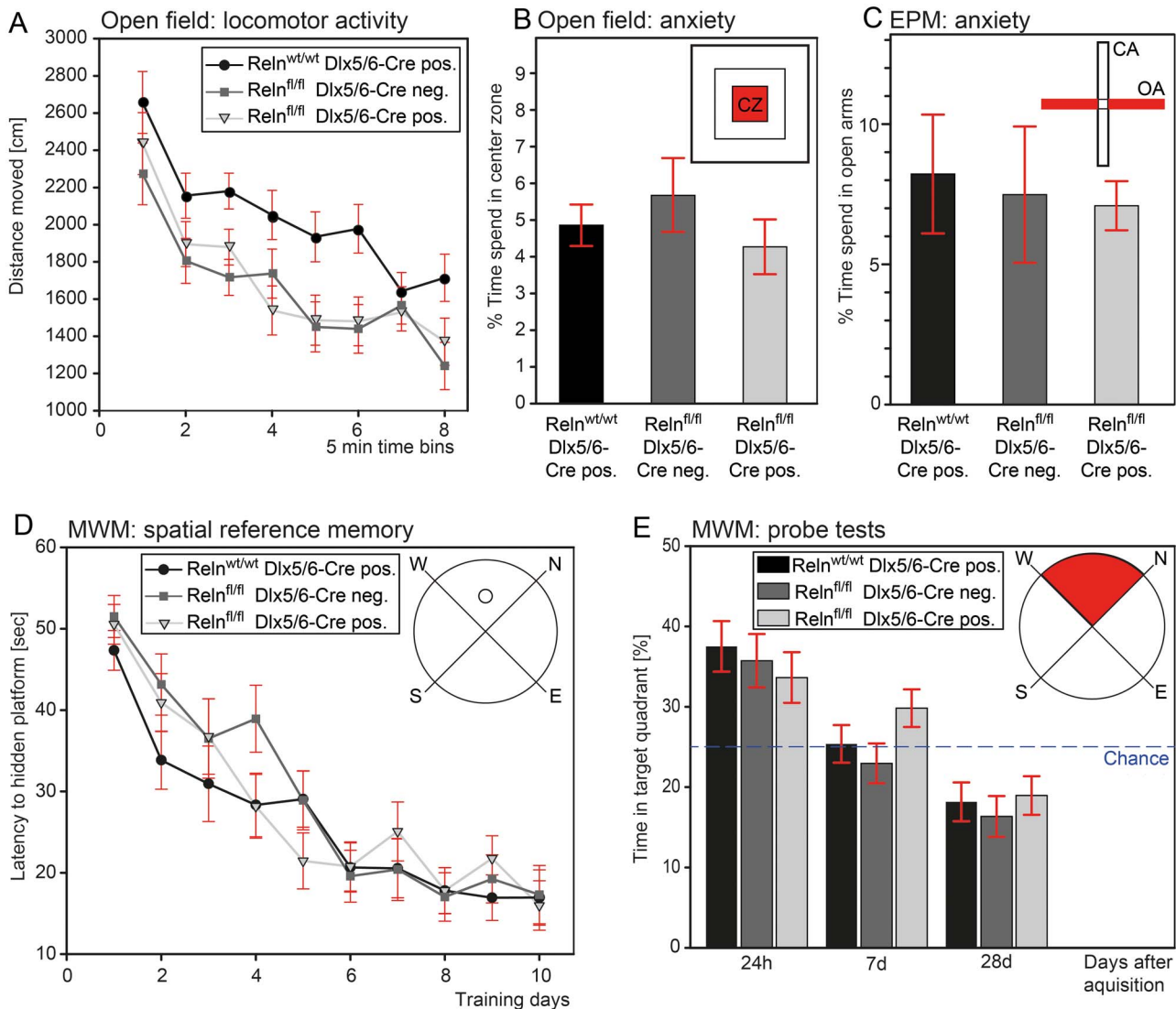


Figure 6. IN-specific Reelin knockout mice showed normal general behavior and intact learning and memory function. (A) Assessment of the distance traveled over a 40 min test session shows unaltered locomotor habituation (time bins: $F(4.21, 113.56) = 32.6$, $P < 0.0001$), but overall more activity in Cre-positive $Rein^{wt/wt}$ mice (genotype: $F(2, 27) = 7.52$, $P < 0.01$). Activity levels were comparable between IN-specific Reelin knockout and Cre-negative $Rein^{fl/fl}$ mice (Bonferroni correction pairwise comparisons: $P = 1.0$). Anxiety-related behavior in terms of time spent in the center of the OF (B) and open arms of the elevated plus maze (EPM) (C) is unaltered in IN-specific Reelin knockout mice. One-way ANOVA (OF: $F(2, 29) = 0.79$, $P = 0.46$; EPM: $F(2, 29) = 0.089$, $P = 0.92$). $N = 10$ mice per group. (D–E) In the MWM task, IN-specific Reelin knockout mice demonstrate intact spatial reference memory acquisition (days: $F(9, 234) = 37.27$, $P < 0.0001$; genotype: $F(2, 26) = 0.62$, $P = 0.54$) and subsequent time-dependent bias for the training quadrant (delay: $F(1.49, 38.62) = 22.86$, $P < 0.0001$; genotype: $F(2, 26) = 1.93$, $P = 0.17$). $N = 9–10$ mice per group. All values represent mean \pm SEM.

Discussion

INs are a major source of Reelin in the adult brain (Pesold et al. 1998); this is confirmed by our WB data. INs contribute about 95% of total Reelin in the adult NC and about 50% of total Reelin in the adult HC. This is consistent with the presence of a substantial number of Reelin-expressing CR cells in the adult HC (Drakew et al. 1998; Anstötz et al. 2016), but not in the adult NC (Chowdhury et al. 2010). In this study, we demonstrate that selective genetic depletion of IN-derived Reelin neither contributes to Reelin's developmental role in neuronal layering (Ogawa et al. 1995) nor to a potential role in layer maintenance (Frotscher et al. 2009) in the dentate gyrus and NC. Our data reveal only subtle effects on adult neurogenesis in the dentate gyrus and show

that learning and memory, such as spatial reference memory, remain unaffected upon depletion of Reelin protein expression, specifically in INs.

A closer look at the dentate gyrus of IN-specific Reelin knockout mice revealed increased numbers of Reelin-expressing CR cells. This suggests that reduced IN-derived Reelin levels might be compensated for by other Reelin-expressing cell types. Yet, despite this increase in Reelin-expressing CR cells in the dentate gyrus, IN-specific Reelin knockout mice show several subtle alterations in this region: Calretinin expression in mossy cells and CB1 receptor levels in the iML were increased, while GFAP intermediate filaments in dentate gyrus astrocytes were

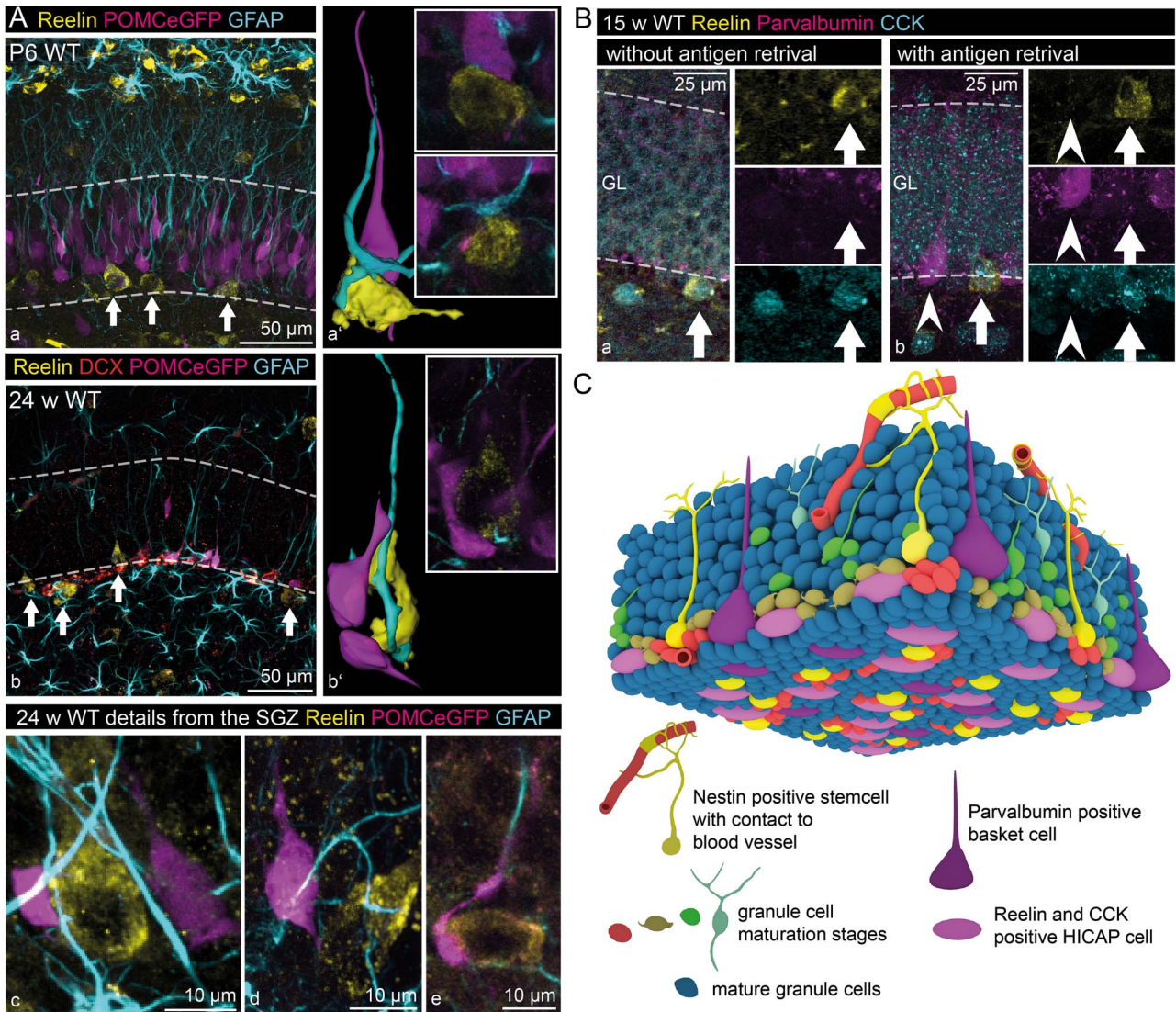


Figure 7. Reelin-expressing inhibitory INs within the stem cell niche. (A) Reelin-expressing INs (white arrows) could be found within the SGZ of the dentate gyrus of young (P6 – a, a') and adult mice (24 weeks – b, b'). Immunohistochemical staining for Reelin, glial fibrillary acidic protein (GFAP, labeling glial cells including RGLCs, Doublecortin (DCX), and POMCeGFP (Overstreet et al. 2004) (both labeling immature neurons) revealed close contact between Reelin-expressing INs, RGLCs, and immature neurons (Images a–e and 3D-reconstructions a', b'). (B) Immunohistochemical stainings of adult (15 weeks) wild-type mice for Reelin, Parvalbumin (marker for basket cells) and CCK (marker for HICAP cells) in the SGZ (staining performed without (a) and with acidic antigen retrieval (b)). The staining revealed coexpression of Reelin and CCK in INs (full arrows), while the Parvalbumin-positive cells were never immunoreactive for Reelin (arrowheads). (C) A representative scheme depicts the observed integration of Reelin-expressing INs within the subgranular stem cell niche (general morphology of the stem cell niche based on data by Fuentealba et al. (2012) and Kempermann et al. (2015)).

reduced. Thus, Reelin derived from INs conveys some specific effects, which could not even be compensated for by increased Reelin expression from other sources.

No Effects on Neuronal Layering and Animal Behavior, Including Learning Ability, and Only Marginal Effects on Adult Neurogenesis in the Dentate Gyrus

Reelin plays an important role in neuronal lamination during brain development (reviewed by Hirota and Nakajima 2017) and is also proposed to play a role in layer maintenance in the adult brain (Frotscher et al. 2009). While it had been shown that CR cells are the most important source of Reelin during forebrain development, it was unclear whether Reelin from

inhibitory INs contributed to Reelin's function in layer formation or maintenance. Reelin expression in INs starts around birth (Schiffmann et al. 1997; Alcantara et al. 1998), a timepoint when neuronal migration and layer formation in the dentate gyrus is still incomplete (Stanfield and Cowan 1979; Altman and Bayer 1990). Our analysis of IN-specific Reelin knockout mice in this study revealed normal neuronal layering in the NC and dentate gyrus, suggesting that Reelin expression in INs is either not required for these processes or might be compensated by functional homologs.

Previous studies have shown that TLE is accompanied by a loss of INs and thus a loss of Reelin-expressing cells in the hilus (Dudek and Shao 2003; Haas and Frotscher 2009). As the lack of Reelin in *reeler* mutant mice leads to a developmental dispersion

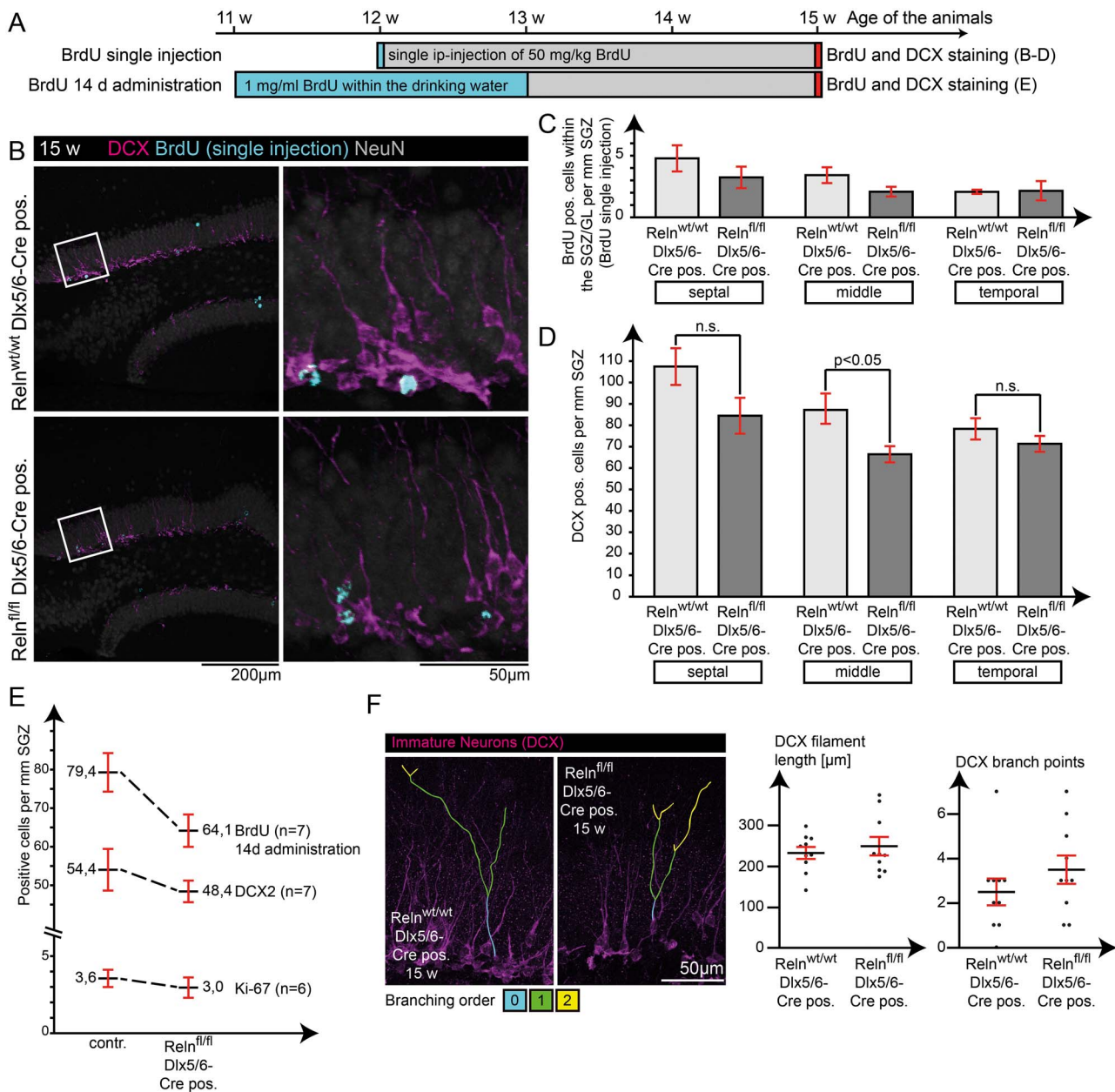


Figure 8. Effect of Reelin from INs on adult neurogenesis. Potential effects on adult neurogenesis were analyzed using BrdU to label newborn granule cells, as well as IHC for Ki-67 (proliferation) and Doublecortin (immature neurons). (A) Application scheme for BrdU in two independent experiments. Visualization (B) and quantification of BrdU-positive cells (C) and Doublecortin-positive cells (D) in slices from septal, middle, and temporal areas of the HC for the single-injection protocol. Only cells within the SGZ and granule cell layer were counted, and cell counts were normalized to the underlying length of the proliferative zone (SGZ) by giving the numbers as “cells per mm SGZ.” Only counts for Doublecortin-positive immature neurons in middle areas of the HC revealed a significant reduction (t-test; $N = 5$; age: 15 weeks; error: \pm SEM) (D). (E) Additional experiments regarding either proliferation (Ki-67 staining and quantification) or neurogenesis (DCX and BrdU quantification for the 14 day BrdU protocol) showed a reduction of about 10% in cell numbers in the IN-specific Reelin knockout mouse, but these differences were not statistically significant. (F) In addition, filament length, orientation, and branching of Doublecortin-positive neurons were not affected in IN-specific knockout mice (t-test; $N = 10$ cells from five animals; age: 15 weeks; error: \pm SEM).

of granule cells, it has been suggested that the lack of Reelin in TLE might be the cause of the observed granule cell dispersion (Haas and Frotscher 2009; Tinnes et al. 2013). However, our data show that Reelin depletion in INs does not lead to granule cell dispersion. As acutely injected Reelin was shown to exert a protective function in kainate injection models of TLE (Müller et al. 2009; Orcinha et al. 2016), we cannot rule out that granule

cell dispersion might be prevented by the increase in Reelin-expressing CR cells around the hippocampal fissure, which we observed in IN-specific Reelin knockout mice.

Reelin is assumed to play a role in adult neurogenesis. By counting BrdU-labeled, DCX- or Ki-67-immunoreactive cells, adult neurogenesis was shown to be decreased by 70–90% in *reeler* mice in several studies (Won et al. 2006; Zhao et al. 2007;

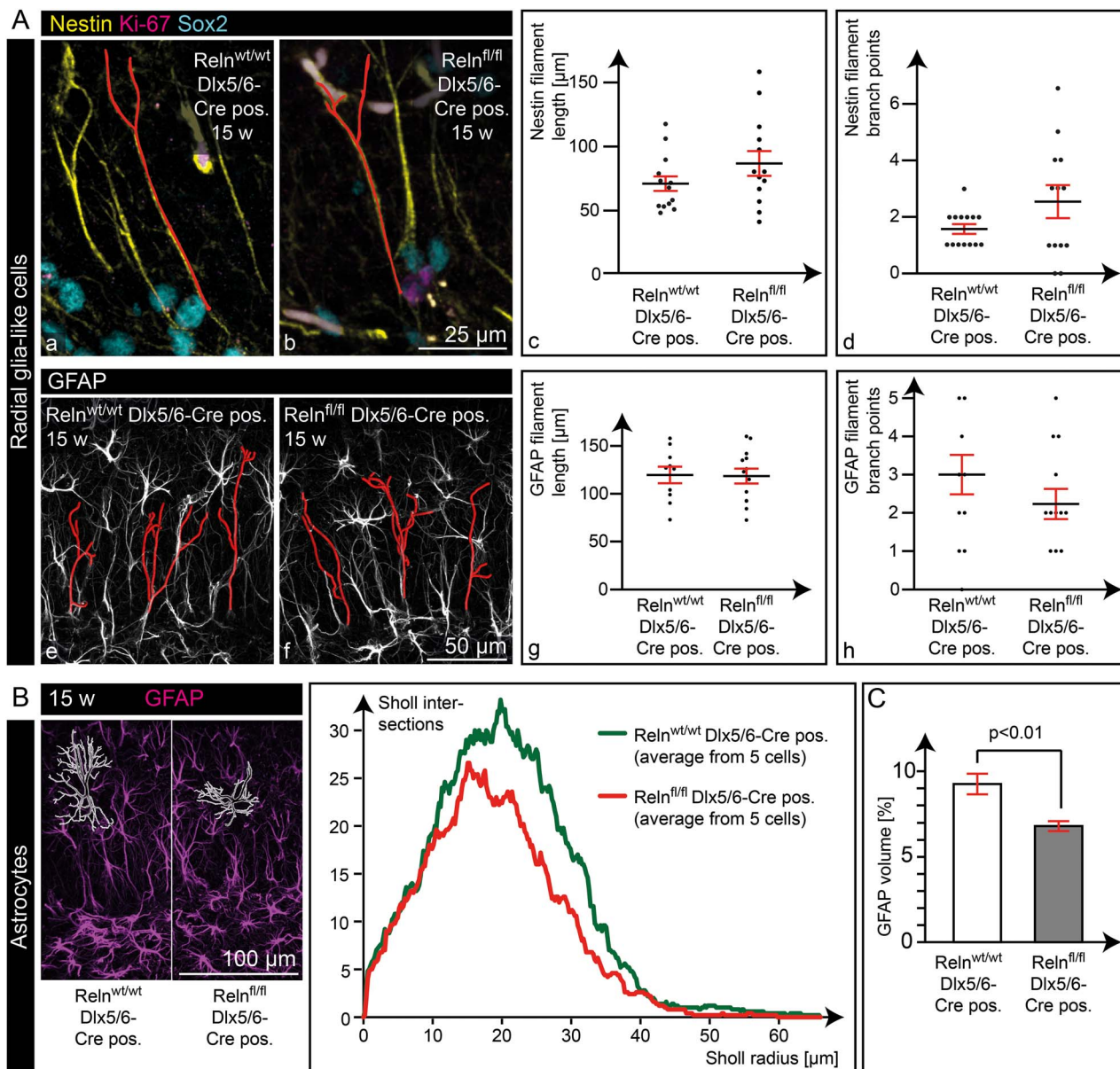


Figure 9. RGLCs and astrocytes in IN-specific Reelin knockout mice. (A) Morphological analysis of the Nestin- (a–d) and GFAP-positive (e–h) intermediate filaments in RGLCs, identified by their prominent radial process spanning through the granule cell layer, revealed normal length (c, g) and branching patterns (d, h) of these filaments (t-test; $N \geq 10$ cells from five animals; age: 15 weeks; error: \pm SEM). Nestin was counterstained with an antibody against transcription factor Sox2 (expressed in undifferentiated stem cells including RGLCs) and Ki-67 (expressed in proliferating cells), to more easily confine the Nestin filament starting point at the soma. (B) Volume reconstruction and Sholl intersections of GFAP filaments from single astrocytes in the ML (depicted is the mean from five cells sampled from five animals; age: 15 weeks). (C) Quantitative measurements of total GFAP filament volume in this area revealed a significant decrease in IN-specific Reelin knockout mice. These data indicate a decrease of astrocytic GFAP filaments in IN-specific Reelin knockout mice (t-test; $N = 5$ animals; age: 15 weeks; error: \pm SEM).

Sibbe et al. 2015). Conversely, overexpression of Reelin within a normally developed dentate gyrus enhanced adult neurogenesis by roughly 23% (BrdU and DCX, Pujadas et al. 2010). Here, we show that numerous Reelin-expressing INs are localized within the neurogenic niche of the dentate gyrus, with tight contact to immature granule cells and RGLCs. We identified these Reelin-expressing IN in the SGZ as CCK-positive HICAP cells, while Parvalbumin-positive basket cells, known to influence neurogenesis (Moss and Toni 2013), were devoid of Reelin expression. Knockout of Reelin from INs resulted in a slight but

consistent decrease in adult neurogenesis of about 10%. Hence, Reelin from INs, although optimally localized to affect stem cell behavior within the stem cell niche, is likely to mediate a very subtle role in the regulation of adult neurogenesis.

Reelin signaling in the adult brain has been shown to modulate synaptic transmission in different ways (Liu et al. 2001; Weeber et al. 2002; Beffert et al. 2005; Chen et al. 2005; Groc et al. 2007; Niu et al. 2008; Campo et al. 2009; Leemhuis et al. 2010; Hellwig et al. 2011; Bal et al. 2013), and heterozygous *reeler* mice show mild behavioral deficits (Tueting et al. 1999;

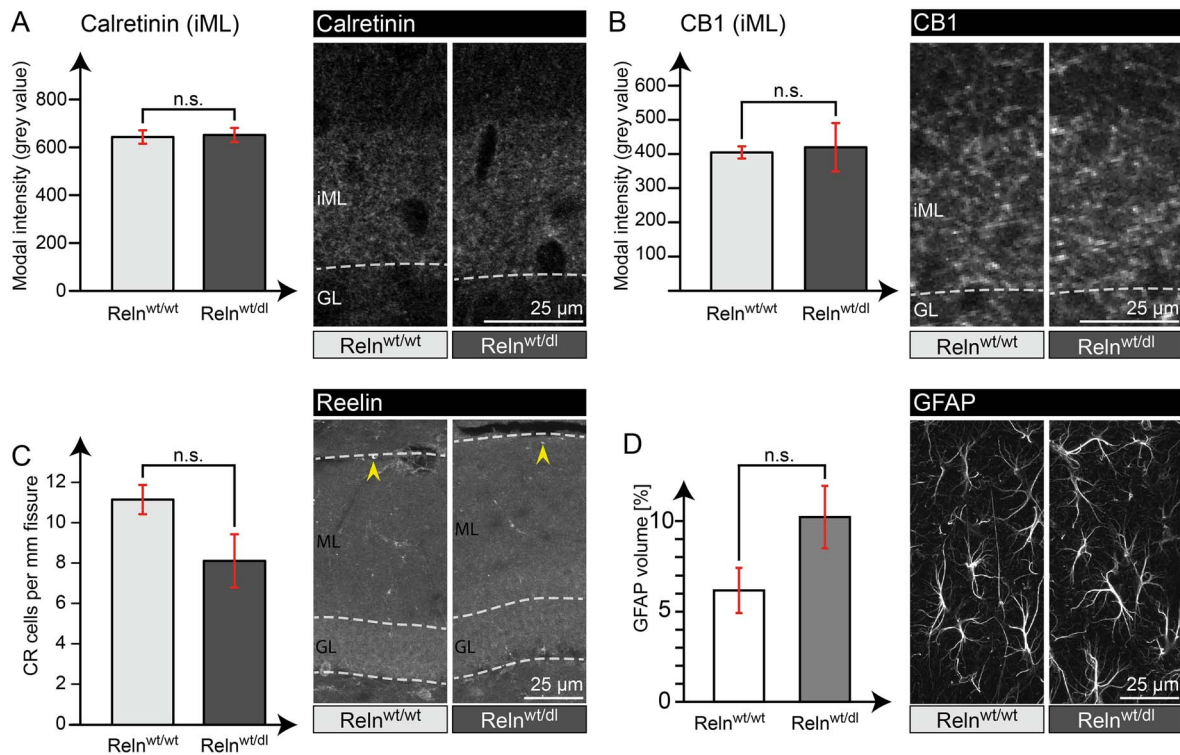


Figure 10. Effects found in IN-specific Reelin knockout mice were not mimicked in heterozygous $Reeln^{wt/dl}$ animals. Analysis of Calretinin (A) and CB1 (B) immunoreactivity within the iML of $Reeln^{wt/dl}$ and $Reeln^{wt/wt}$ animals revealed comparable intensity levels in both genotypes. In addition, quantification of Reelin-expressing CR cells around the hippocampal fissure (yellow arrowheads) (C) showed a tendency to reduced numbers (not significant) and analysis of GFAP filaments (D) a tendency to increased levels (not significant) in $Reeln^{wt/dl}$ mice, compared with $Reeln^{wt/wt}$ (t-test; $N = 4$ animals; age: 24 weeks; error: \pm SEM).

Rogers et al. 2013). Although IN-specific Reelin knockout mice demonstrate less Reelin expression in the adult brain compared with heterozygous *reeler* mice, we did not observe behavioral alterations with respect to exploratory drive and locomotor activity, anxiety-related behavior and spatial learning and memory. This does not necessarily rule out subtle synaptic changes, which are not readily detected at the behavioral level in terms of altered learning and memory.

In addition, some of Reelin's effects only manifest under pathological conditions. For example, global loss of Reelin precipitates learning and memory deficits in an Alzheimer disease model (Lane-Donovan et al. 2015). Along these lines, corticosterone-induced stress results in spatial memory deficits in heterozygous *reeler* mice, but not in wild-type animals (Schroeder et al. 2015; Notaras et al. 2017). The effects of Reelin on synapse function may therefore become more pronounced under pathophysiological conditions.

Thus, although IN-specific Reelin knockout mice demonstrate intact learning and memory under the specific conditions described in our study, a detailed assessment of synaptic function, and the degree to which additional factors such as stress might precipitate cognitive deficits in this mouse model warrants further investigation.

Phenotype of Interneuron-Specific Reelin Knockout Mice

In the IN-specific Reelin knockout mouse, we identified a significant increase in Reelin-expressing CR cells surrounding the hippocampal fissure, thus pointing to an autocrine fashion of Reelin signaling in CR cells. It is tempting to speculate

that an increase in the number of Reelin-expressing CR cells might compensate for the loss of Reelin-expressing IN. Notably, the number of IN which lack Reelin expression next to the hippocampal fissure, equals the increase in the number of Reelin-expressing CR cells in this area. As a result, the total number of Reelin-expressing cells remains unaltered in areas next to the hippocampal fissure. This observation is consistent with earlier results showing that CR cells are affected regarding numbers and positioning in classical *reeler* mutant mice (Derer 1985; Coulin et al. 2001; Anstötz et al. 2019). Taken together, we conclude that an autocrine effect of Reelin on CR cells may be a possibility that requires further investigation.

Our study also identified increased Calretinin expression in hilar mossy cells and increased Calretinin and CB1 levels in the iML. Calretinin is a calcium-binding protein believed to act as a slow or fast onset buffer, depending on the intracellular Ca^{2+} concentration (reviewed in Schwaller 2014). It plays a role in dentate gyrus long-term potentiation (Schurmans et al. 1997; Gurden et al. 1998) and may also be important in protecting cells from excitotoxicity (Camp and Wijesinghe 2009). The CB1 receptor is one of two so far identified cannabinoid receptors. In the forebrain, the CB1 receptor is enriched in axons and presynaptic terminals and its expression is highly correlated to INs containing CCK (Mackie 2006), which we found to be Reelin-positive in the dentate gyrus. Functionally, CB1 receptors inhibit neurotransmitter release and are involved in long-term depression (Freund et al. 2003; Lutz 2004). So far, no functional connection between Reelin, Calretinin and CB1 has been described, apart from the fact that they are partly coexpressed in the same cells (Hevner et al. 2003; Morozov et al. 2009; Gonzalez-Gomez and Meyer 2014).

In addition, GFAP, a glial cell-specific intermediate filament (Schnitzer et al. 1981; Ogata and Kosaka 2002), was found to be reduced in astrocytes of the dentate gyrus. A recent study has shown that Reelin overexpression leads to reduced neuron-glia contact at the synapse, while knockout of Dab1, and thus intracellular interruption of the canonical Reelin signaling cascade, results in enhanced enwrapping of synapses with glial processes (Bosch et al. 2016). This fits in well with observations during brain development, where Reelin is important in the release of neurons from radial glial cells (Sanada et al. 2004). From this finding, one assumption is that a decrease in Reelin levels should lead to increased neuron-glia contact and accordingly, a more complex morphology of astrocytes. On the other hand, it has been shown that GFAP-positive cells grow preferentially on Reelin-coated stripes (Förster et al. 2002), and glial endfeet of radial glial cells require Reelin to attach to the ML in the NC (Hartfuss et al. 2003) and to the basement membrane in the spinal cord (Lee and Song 2013). Thus, lack of Reelin results in a slightly reduced length of glial processes, which is consistent with the reduction in GFAP filament complexity in IN-specific Reelin knockout mice. This might interfere with the formation of tripartite synapses in the areas, which are commonly occupied by the outermost glial processes. This hypothesis, too, shows that further studies on synaptic function in the IN-specific Reelin knockout mouse might be a promising approach.

Of note, all pronounced effects in the dentate gyrus are found in the ML, despite the fact that Reelin-expressing CR cells are located at the hippocampal fissure and hence in close vicinity to this area. This finding suggests different functions of Reelin, depending on its origin, either from CR cells or INs. One could argue that there is no reason to expect that Reelin from these alternative sources would act in different ways, as in both cases it is secreted into the extracellular matrix (ECM) (D'Arcangelo et al. 1995, 1997; Campo et al. 2009) and may act over some distance. However, it needs to be considered that Reelin is a large 450 kDa protein (D'Arcangelo et al. 1995; Jossin et al. 2007), which dimerizes after secretion (Utsunomiya-Tate et al. 2000; Kubo et al. 2002) and acts locally in the vicinity of secreting cells (Koie et al. 2014). Furthermore, Reelin binds to other ECM components (Panteri et al. 2006; Tan et al. 2008) and only fragments of Reelin, produced by proteolytical cleavage (Jossin et al. 2007; Yasui et al. 2007), might be able to diffuse over larger distances. Previous studies showed that Reelin fragments functionally differ from full-length Reelin (Schmid et al. 2005; Jossin et al. 2007; Nakano et al. 2007; Hibi and Hattori 2009; Kohno et al. 2009; Bouché et al. 2013). In addition, Reelin in CR cells was also shown to be secreted from axons (Derer et al. 2001). In light of these observations, INs appear to be suitable to distribute full-length Reelin within the ML due to their characteristic elaborated axon plexus.

Overall, the subtle changes observed in the dentate gyrus, a brain area where Reelin is expressed by INs as well as CR cells, indicate that there is a specific function of Reelin from INs, which cannot be compensated by Reelin from other sources.

Supplementary Material

Supplementary material is available at *Cerebral Cortex* online.

Funding

This work was supported by the Deutsche Forschungsgemeinschaft (BR4888 2-1, BR4888 4-2 to B.B. and Fro620 12-2, Fro620

13-1, FOR2419 Fro620 14-1 to M.F., SFB 974/19058643 to H.H.B., FOR2419/KN556 11-2 to M.K.); the Hertie Foundation (Senior Research Professorship to M.F.); Landesforschungsförderung Hamburg (LEF-FV27b to M.F.); and the National Institute of Health (R37 HL63761, R01 NS093382, R01 NS108115, RF1 AG053391 to J.H.). In addition, JH is supported by the Consortium for Frontotemporal Dementia Research and the Bright Focus Foundation.

Notes

We thank Alf Neu for 3D modeling of the stem cell niche with Adobe Illustrator CC22.12018 and Autodesk 3Ds max 2018, and Hans Jörg Fehling and Gary Westbrook for providing tdRFP-reporter and POMCeGFP mice, respectively. We thank Bettina Herde, Dung Ludwig, Dagmar Drexler for genotyping; Saskia Siegel, Helga Herbolt, and Christiane Schröder for technical support; Silvana Deutsch and Kristian Schacht for animal care; Hiltrud Voss and Eva Kronberg for technical support and animal care; and Irm Hermans-Borgmeyer at the ZMNH core facility for the transgenic mice. *Conflict of Interest*: None declared

References

- Alcantara S, Ruiz M, D'Arcangelo G, Ezan F, de Lecea L, Curran T, Sotelo C, Soriano E. 1998. Regional and cellular patterns of Reelin mRNA expression in the forebrain of the developing and adult mouse. *J Neurosci*. 18:7779–7799.
- Altman J, Bayer SA. 1990. Migration and distribution of two populations of hippocampal granule cell precursors during the perinatal and postnatal periods. *J Comp Neurol*. 301: 365–381.
- Anstötz M, Huang H, Marchionni I, Haumann I, Maccaferri G, Lubke JH. 2016. Developmental profile, morphology, and synaptic connectivity of Cajal-Retzius cells in the postnatal mouse hippocampus. *Cereb Cortex*. 26:855–872.
- Anstötz M, Karsak M, Rune GM. 2019. Integrity of Cajal-Retzius cells in the Reeler-mouse hippocampus. *Hippocampus*. 29:550–565.
- Bal M, Leitz J, Reese AL, Ramirez DM, Durakoglugil M, Herz J, Monteggia LM, Kavalali ET. 2013. Reelin mobilizes a VAMP7-dependent synaptic vesicle pool and selectively augments spontaneous neurotransmission. *Neuron*. 80:934–946.
- Bannerman DM, Sprengel R, Sanderson DJ, McHugh SB, Rawlins JN, Monyer H, Seeburg PH. 2014. Hippocampal synaptic plasticity, spatial memory and anxiety. *Nat Rev Neurosci*. 15:181–192.
- Beffert U, Weeber EJ, Durudas A, Qiu S, Masiulis I, Sweatt JD, Li WP, Adelman G, Frotscher M, Hammer RE et al. 2005. Modulation of synaptic plasticity and memory by Reelin involves differential splicing of the lipoprotein receptor Apoer2. *Neuron*. 47:567–579.
- Bielle F, Griveau A, Narboux-Neme N, Vigneau S, Sigris M, Arber S, Wassef M, Pierani A. 2005. Multiple origins of Cajal-Retzius cells at the borders of the developing pallidum. *Nat Neurosci*. 8:1002–1012.
- Bock HH, May P. 2016. Canonical and non-canonical Reelin signaling. *Front Cell Neurosci*. 10:166.
- Boncinelli E. 1994. Early CNS development: distal-less related genes and forebrain development. *Curr Opin Neurobiol*. 4:29–36.
- Bosch C, Masachs N, Exposito-Alonso D, Martinez A, Teixeira CM, Fernaud I, Pujadas L, Ulloa F, Comella JX, DeFelipe J et al.

2016. Reelin regulates the maturation of dendritic spines, synaptogenesis and glial ensheathment of newborn granule cells. *Cereb Cortex*. 26:4282–4298.
- Bouché E, Romero-Ortega MI, Henkemeyer M, Catchpole T, Leemhuis J, Frotscher M, May P, Herz J, Bock HH. 2013. Reelin induces EphB activation. *Cell Res*. 23:473–490.
- Boyle MP, Bernard A, Thompson CL, Ng L, Boe A, Mortrud M, Hawrylycz MJ, Jones AR, Hevner RF, Lein ES. 2011. Cell-type-specific consequences of Reelin deficiency in the mouse neocortex, hippocampus, and amygdala. *J Comp Neurol*. 519:2061–2089.
- Brunkhorst R, Bock H, Derouiche A. 2015. Reelin induces process growth in cultured astrocytes: implication for glia-synaptic plasticity. *Arch Ital Biol*. 153:249–254.
- Brunne B, Franco S, Bouché E, Herz J, Howell BW, Pahle J, Muller U, May P, Frotscher M, Bock HH. 2013. Role of the postnatal radial glial scaffold for the development of the dentate gyrus as revealed by Reelin signaling mutant mice. *Glia*. 61:1347–1363.
- Brunne B, Zhao S, Derouiche A, Herz J, May P, Frotscher M, Bock HH. 2010. Origin, maturation, and astroglial transformation of secondary radial glial cells in the developing dentate gyrus. *Glia*. 58:1553–1569.
- Camp AJ, Wijesinghe R. 2009. Calretinin: modulator of neuronal excitability. *Int J Biochem Cell Biol*. 41:2118–2121.
- Campo CG, Sinagra M, Verrier D, Manzoni OJ, Chavis P. 2009. Reelin secreted by GABAergic neurons regulates glutamate receptor homeostasis. *PLoS One*. 4:e5505.
- Chai X, Munzner G, Zhao S, Tinnes S, Kowalski J, Haussler U, Young C, Haas CA, Frotscher M. 2014. Epilepsy-induced motility of differentiated neurons. *Cereb Cortex*. 24:2130–2140.
- Chen Y, Beffert U, Ertunc M, Tang TS, Kavalali ET, Bezprozvanny I, Herz J. 2005. Reelin modulates NMDA receptor activity in cortical neurons. *J Neurosci*. 25:8209–8216.
- Chowdhury TG, Jimenez JC, Bomar JM, Cruz-Martin A, Cantle JP, Portera-Cailliau C. 2010. Fate of Cajal-Retzius neurons in the postnatal mouse neocortex. *Front Neuroanat*. 4:10.
- Costa E, Chen Y, Davis J, Dong E, Noh JS, Tremolizzo L, Veldic M, Grayson DR, Guidotti A. 2002. REELIN and schizophrenia: a disease at the interface of the genome and the epigenome. *Mol Interv*. 2:47–57.
- Coulin C, Drakew A, Frotscher M, Deller T. 2001. Stereological estimates of total neuron numbers in the hippocampus of adult Reeler mutant mice: evidence for an increased survival of Cajal-Retzius cells. *J Comp Neurol*. 439:19–31.
- D’Arcangelo G, Miao GG, Chen SC, Soares HD, Morgan JI, Curran T. 1995. A protein related to extracellular matrix proteins deleted in the mouse mutant Reeler. *Nature*. 374:719–723.
- D’Arcangelo G, Nakajima K, Miyata T, Ogawa M, Mikoshiba K, Curran T. 1997. Reelin is a secreted glycoprotein recognized by the CR-50 monoclonal antibody. *J Neurosci*. 17:23–31.
- D’Arcangelo G. 2006. Reelin mouse mutants as models of cortical development disorders. *Epilepsy Behav*. 8:81–90.
- Drakew A, Frotscher M, Deller T, Ogawa M, Heimrich B. 1998. Developmental distribution of a Reeler gene-related antigen in the rat hippocampal formation visualized by CR-50 immunocytochemistry. *Neuroscience*. 82:1079–1086.
- Derer P. 1985. Comparative localization of Cajal-Retzius cells in the neocortex of normal and Reeler mutant mice fetuses. *Neurosci Lett*. 54:1–6.
- Derer P, Derer M, Goffinet A. 2001. Axonal secretion of Reelin by Cajal-Retzius cells: evidence from comparison of normal and Reelin (Orl) mutant mice. *J Comp Neurol*. 440:136–143.
- Dudek FE, Shao LR. 2003. Loss of GABAergic interneurons in seizure-induced epileptogenesis. *Epilepsy Curr*. 3:159–161.
- Falconer DS. 1951. Two new mutants ‘Trembler’ and ‘Reeler’, with neurological actions in the house mouse. *J Genetics*. 50:192–201.
- Fatemi SH. 2001. Reelin mutations in mouse and man: from Reeler mouse to schizophrenia, mood disorders, autism and lissencephaly. *Mol Psychiatry*. 6:129–133.
- Fatemi SH, Earle JA, McMenomy T. 2000. Reduction in Reelin immunoreactivity in hippocampus of subjects with schizophrenia, bipolar disorder and major depression. *Mol Psychiatry*. 5:654–663, 571.
- Feng G, Mellor RH, Bernstein M, Keller-Peck C, Nguyen QT, Wallace M, Nerbonne JM, Lichtman JW, Sanes JR. 2000. Imaging neuronal subsets in transgenic mice expressing multiple spectral variants of GFP. *Neuron*. 28:41–51.
- Förster E, Tielsch A, Saum B, Weiss KH, Johanssen C, Graus-Porta D, Muller U, Frotscher M. 2002. Reelin, disabled 1, and beta 1 integrins are required for the formation of the radial glial scaffold in the hippocampus. *Proc Natl Acad Sci U S A*. 99:13178–13183.
- Francis F, Koulikoff A, Boucher D, Chafey P, Schaar B, Vinet MC, Riocourt G, McDonnell N, Reiner O, Kahn A et al. 1999. Doublecortin is a developmentally regulated, microtubule-associated protein expressed in migrating and differentiating neurons. *Neuron*. 23:247–256.
- Freund TF, Buzsaki G. 1996. IN of the hippocampus. *Hippocampus*. 6:347–470.
- Freund TF, Katona I, Piomelli D. 2003. Role of endogenous cannabinoids in synaptic signaling. *Physiol Rev*. 83:1017–1066.
- Frotscher M, Chai X, Bock HH, Haas CA, Förster E, Zhao S. 2009. Role of Reelin in the development and maintenance of cortical lamination. *J Neural Transm*. 116:1451–1455.
- Frotscher M, Haas CA, Förster E. 2003. Reelin controls granule cell migration in the dentate gyrus by acting on the radial glial scaffold. *Cereb Cortex*. 13:634–640.
- Fuentealba LC, Obernier K, Alvarez-Buylla A. 2012. Adult neural stem cells bridge their niche. *Cell Stem Cell*. 10:698–708.
- Gonzalez-Gomez M, Meyer G. 2014. Dynamic expression of calretinin in embryonic and early fetal human cortex. *Front Neuroanat*. 8:41.
- Groc L, Choquet D, Stephenson F, Verrier D, Manzoni O, Chavis P. 2007. NMDA receptor surface trafficking and synaptic subunit composition are developmentally regulated by the extracellular matrix protein Reelin. *J Neurosci*. 27:10165–10175.
- Guidotti A, Auta J, Davis JM, Di-Giorgi-Gerevini V, Dwivedi Y, Grayson DR, Impagnatiello F, Pandey G, Pesold C, Sharma R et al. 2000. Decrease in Reelin and glutamic acid decarboxylase67 (GAD67) expression in schizophrenia and bipolar disorder: a postmortem brain study. *Arch Gen Psychiatry*. 57:1061–1069.
- Gurden H, Schiffmann SN, Lemaire M, Bohme GA, Parmentier M, Schurmans S. 1998. Calretinin expression as a critical component in the control of dentate gyrus long-term potentiation induction in mice. *Eur J Neurosci*. 10:3029–3033.
- Haas CA, Dudeck O, Kirsch M, Huszka C, Kann G, Pollak S, Zentner J, Frotscher M. 2002. Role for Reelin in the development of granule cell dispersion in temporal lobe epilepsy. *J Neurosci*. 22:5797–5802.
- Haas CA, Frotscher M. 2009. Reelin deficiency causes granule cell dispersion in epilepsy. *Exp Brain Res*. 200:141–149.
- Hartfuss E, Förster E, Bock HH, Hack MA, LePrince P, Luque JM, Herz J, Frotscher M, Gotz M. 2003. Reelin signaling directly

- affects radial glia morphology and biochemical maturation. *Development*. 130:4597–4609.
- Hellwig S, Hack I, Kowalski J, Brunne B, Jarowyj J, Unger A, Bock HH, Junghans D, Frotscher M. 2011. Role for Reelin in neurotransmitter release. *J Neurosci*. 31:2352–2360.
- Hevner RF, Daza RA, Englund C, Kohtz J, Fink A. 2004. Postnatal shifts of interneuron position in the neocortex of normal and Reeler mice: evidence for inward radial migration. *Neuroscience*. 124:605–618.
- Hevner RF, Neogi T, Englund C, Daza RA, Fink A. 2003. Cajal-Retzius cells in the mouse: transcription factors, neurotransmitters, and birthdays suggest a pallial origin. *Brain Res Dev Brain Res*. 141:39–53.
- Hibi T, Hattori M. 2009. The N-terminal fragment of Reelin is generated after endocytosis and released through the pathway regulated by Rab11. *FEBS Lett*. 583:1299–1303.
- Hirota Y, Nakajima K. 2017. Control of neuronal migration and aggregation by Reelin signaling in the developing cerebral cortex. *Front Cell Dev Biol*. 5:40.
- Houser CR. 2007. Interneurons of the dentate gyrus: an overview of cell types, terminal fields and neurochemical identity. *Prog Brain Res*. 163:217–232.
- Ikeda Y, Terashima T. 1997. Expression of Reelin, the gene responsible for the Reeler mutation, in embryonic development and adulthood in the mouse. *Dev Dyn*. 210:157–172.
- Impagnatiello F, Guidotti AR, Pesold C, Dwivedi Y, Caruncho H, Pisu MG, Uzunov DP, Smalheiser NR, Davis JM, Pandey GN et al. 1998. A decrease of Reelin expression as a putative vulnerability factor in schizophrenia. *Proc Natl Acad Sci U S A*. 95:15718–15723.
- Jossin Y, Gui L, Goffinet AM. 2007. Processing of Reelin by embryonic neurons is important for function in tissue but not in dissociated cultured neurons. *J Neurosci*. 27:4243–4252.
- Kee N, Sivalingam S, Boonstra R, Wojtowicz JM. 2002. The utility of Ki-67 and BrdU as proliferative markers of adult neurogenesis. *J Neurosci Methods*. 115:97–105.
- Kempermann G, Song H, Gage FH. 2015. Neurogenesis in the adult hippocampus. *Cold Spring Harb Perspect Biol*. 7:a018812.
- Kohno T, Nakano Y, Kitoh N, Yagi H, Kato K, Baba A, Hattori M. 2009. C-terminal region-dependent change of antibody-binding to the eighth Reelin repeat reflects the signaling activity of Reelin. *J Neurosci Res*. 87:3043–3053.
- Koie M, Okumura K, Hisanaga A, Kamei T, Sasaki K, Deng M, Baba A, Kohno T, Hattori M. 2014. Cleavage within Reelin repeat 3 regulates the duration and range of signaling activity of Reelin. *J Biol Chem*. 289:12922–12930.
- Krueger DD, Howell JL, Hebert BF, Olausson P, Taylor JR, Nairn AC. 2006. Assessment of cognitive function in the heterozygous Reeler mouse. *Psychopharmacology*. 189:95–104.
- Kubo K, Mikoshiba K, Nakajima K. 2002. Secreted Reelin molecules form homodimers. *Neurosci Res*. 43:381–388.
- Lane-Donovan C, Philips GT, Wasser CR, Durakoglugil MS, Masiulis I, Upadhaya A, Pohlkamp T, Coskun C, Kotti T, Steller L et al. 2015. Reelin protects against amyloid beta toxicity in vivo. *Sci Signal*. 8:ra67.
- Lee GH, D'Arcangelo G. 2016. New insights into Reelin-mediated signaling pathways. *Front Cell Neurosci*. 10:122.
- Lee H, Song MR. 2013. The structural role of radial glial endfeet in confining spinal motor neuron somata is controlled by the Reelin and notch pathways. *Exp Neurol*. 249C:83–94.
- Leemhuis J, Bouché E, Frotscher M, Henle F, Hein L, Herz J, Meyer DK, Pichler M, Roth G, Schwan C et al. 2010. Reelin signals through apolipoprotein E receptor 2 and Cdc42 to increase growth cone motility and filopodia formation. *J Neurosci*. 30:14759–14772.
- Liu WS, Pesold C, Rodriguez MA, Carboni G, Auta J, Lacor P, Larson J, Condie BG, Guidotti A, Costa E. 2001. Down-regulation of dendritic spine and glutamic acid decarboxylase 67 expressions in the Reelin haploinsufficient heterozygous Reeler mouse. *Proc Natl Acad Sci U S A*. 98:3477–3482.
- Luche H, Weber O, Nageswara Rao T, Blum C, Fehling HJ. 2007. Faithful activation of an extra-bright red fluorescent protein in "knock-in" Cre-reporter mice ideally suited for lineage tracing studies. *Eur J Immunol*. 37:43–53.
- Lutz B. 2004. On-demand activation of the endocannabinoid system in the control of neuronal excitability and epileptiform seizures. *Biochem Pharmacol*. 68:1691–1698.
- Mackie K. 2006. Mechanisms of CB1 receptor signaling: endocannabinoid modulation of synaptic strength. *Int J Obes*. 30(Suppl 1):S19–S23.
- Miyoshi G, Hjerling-Leffler J, Karayannis T, Sousa VH, Butt SJ, Battiste J, Johnson JE, Machold RP, Fishell G. 2010. Genetic fate mapping reveals that the caudal ganglionic eminence produces a large and diverse population of superficial cortical IN. *J Neurosci*. 30:1582–1594.
- Monory K, Massa F, Egertova M, Eder M, Blaudzun H, Westenbroek R, Kelsch W, Jacob W, Marsch R, Ekker M et al. 2006. The endocannabinoid system controls key epileptogenic circuits in the hippocampus. *Neuron*. 51:455–466.
- Morozov YM, Torii M, Rakic P. 2009. Origin, early commitment, migratory routes, and destination of cannabinoid type 1 receptor-containing IN. *Cereb Cortex*. 19(Suppl 1):i78–i89.
- Moss J, Toni N. 2013. A circuit-based gatekeeper for adult neural stem cell proliferation: Parvalbumin-expressing IN of the dentate gyrus control the activation and proliferation of quiescent adult neural stem cells. *Bioessays*. 35:28–33.
- Müller MC, Osswald M, Tinnes S, Haussler U, Jacobi A, Förster E, Frotscher M, Haas CA. 2009. Exogenous Reelin prevents granule cell dispersion in experimental epilepsy. *Exp Neurol*. 216:390–397.
- Nakano Y, Kohno T, Hibi T, Kohno S, Baba A, Mikoshiba K, Nakajima K, Hattori M. 2007. The extremely conserved C-terminal region of Reelin is not necessary for secretion but is required for efficient activation of downstream signaling. *J Biol Chem*. 282:20544–20552.
- Niu S, Yabut O, D'Arcangelo G. 2008. The Reelin signaling pathway promotes dendritic spine development in hippocampal neurons. *J Neurosci*. 28:10339–10348.
- Notaras MJ, Vivian B, Wilson C, van den Buuse M. 2017. Interaction of Reelin and stress on immobility in the forced swim test but not dopamine-mediated locomotor hyperactivity or prepulse inhibition disruption: relevance to psychotic and mood disorders. *Schizophr Res*. doi:10.1016/j.schres.2017.07.016.
- Nullmeier S, Panther P, Dobrowolny H, Frotscher M, Zhao S, Schwegler H, Wolf R. 2011. Region-specific alteration of GABAergic markers in the brain of heterozygous Reeler mice. *Eur J Neurosci*. 33:689–698.
- Ogata K, Kosaka T. 2002. Structural and quantitative analysis of astrocytes in the mouse hippocampus. *Neuroscience*. 113:221–233.
- Ogawa M, Miyata T, Nakajima K, Yagyu K, Seike M, Ikenaka K, Yamamoto H, Mikoshiba K. 1995. The reeler gene-associated antigen on Cajal-Retzius neurons is a crucial molecule for laminar organization of cortical neurons. *Neuron*. 14:899–912.

- O'Keefe, Nadel. 1978. The hippocampus as a cognitive map. In: *New York (NY): Oxford University Press.*
- Orcinha C, Munzner G, Gerlach J, Kiliyas A, Follo M, Egert U, Haas CA. 2016. Seizure-induced motility of differentiated dentate granule cells is prevented by the central Reelin fragment. *Front Cell Neurosci.* 10:183.
- Overstreet LS, Hentges ST, Bumashny VF, de Souza FS, Smart JL, Santangelo AM, Low MJ, Westbrook GL, Rubinstein M. 2004. A transgenic marker for newly born granule cells in dentate gyrus. *J Neurosci.* 24:3251–3259.
- Panteri R, Paiardini A, Keller F. 2006. A 3D model of Reelin subrepeat regions predicts Reelin binding to carbohydrates. *Brain Res.* 1116:222–230.
- Pesold C, Impagnatiello F, Pisu MG, Uzunov DP, Costa E, Guidotti A, Caruncho HJ. 1998. Reelin is preferentially expressed in neurons synthesizing gamma-aminobutyric acid in cortex and hippocampus of adult rats. *Proc Natl Acad Sci U S A.* 95:3221–3226.
- Pesold C, Liu WS, Guidotti A, Costa E, Caruncho HJ. 1999. Cortical bitufted, horizontal, and Martinotti cells preferentially express and secrete reelin into perineuronal nets, nonsynaptically modulating gene expression. *Proc Natl Acad Sci U S A.* 96:3217–3222.
- Podhorna J, Didriksen M. 2004. The heterozygous Reeler mouse: behavioural phenotype. *Behav Brain Res.* 153:43–54.
- Pohlkamp T, David C, Cauli B, Gallopin T, Bouché E, Karagiannis A, May P, Herz J, Frotscher M, Staiger JF et al. 2014. Characterization and distribution of Reelin-positive IN subtypes in the rat barrel cortex. *Cereb Cortex.* 24:3046–3058.
- Pujadas L, Gruart A, Bosch C, Delgado L, Teixeira CM, Rossi D, de Lecea L, Martinez A, Delgado-Garcia JM, Soriano E. 2010. Reelin regulates postnatal neurogenesis and enhances spine hypertrophy and long-term potentiation. *J Neurosci.* 30:4636–4649.
- Rakic P, Caviness VS Jr. 1995. Cortical development: view from neurological mutants two decades later. *Neuron.* 14:1101–1104.
- Rogers J, Zhao L, Trotter J, Rusiana I, Peters M, Li Q, Donaldson E, Banko J, Keenoy K, Rebeck G et al. 2013. Reelin supplementation recovers sensorimotor gating, synaptic plasticity and associative learning deficits in the heterozygous Reeler mouse. *J Psychopharmacol.* 27:386–395.
- Ruest LB, Hammer RE, Yanagisawa M, Clouthier DE. 2003. Dlx5/6-enhancer directed expression of Cre recombinase in the pharyngeal arches and brain. *Genesis.* 37:188–194.
- Sanada K, Gupta A, Tsai LH. 2004. Disabled-1-regulated adhesion of migrating neurons to radial glial fiber contributes to neuronal positioning during early corticogenesis. *Neuron.* 42:197–211.
- Schiffmann SN, Bernier B, Goffinet AM. 1997. Reelin mRNA expression during mouse brain development. *Eur J Neurosci.* 9:1055–1071.
- Schindelin J, Arganda-Carreras I, Frise E, Kaynig V, Longair M, Pietzsch T, Preibisch S, Rueden C, Saalfeld S, Schmid B et al. 2012. Fiji: an open-source platform for biological-image analysis. *Nat Methods.* 9:676–682.
- Schmid RS, Jo R, Shelton S, Kreidberg JA, Anton ES. 2005. Reelin, integrin and DAB1 interactions during embryonic cerebral cortical development. *Cereb Cortex.* 15:1632–1636.
- Schneider CA, Rasband WS, Eliceiri KW. 2012. NIH image to ImageJ: 25 years of image analysis. *Nat Methods.* 9:671–675.
- Schnitzer J, Franke WW, Schachner M. 1981. Immunocytochemical demonstration of vimentin in astrocytes and ependymal cells of developing and adult mouse nervous system. *J Cell Biol.* 90:435–447.
- Schroeder A, Buret L, Hill RA, van den Buuse M. 2015. Gene-environment interaction of Reelin and stress in cognitive behaviours in mice: implications for schizophrenia. *Behav Brain Res.* 287:304–314.
- Schurmans S, Schiffmann SN, Gurden H, Lemaire M, Lipp HP, Schwam V, Pochet R, Imperato A, Bohme GA, Parmentier M. 1997. Impaired long-term potentiation induction in dentate gyrus of calretinin-deficient mice. *Proc Natl Acad Sci U S A.* 94:10415–10420.
- Schwaller B. 2014. Calretinin: from a "simple" Ca(2+) buffer to a multifunctional protein implicated in many biological processes. *Front Neuroanat.* 8:3.
- Schwenk F, Baron U, Rajewsky K. 1995. A cre-transgenic mouse strain for the ubiquitous deletion of loxP-flanked gene segments including deletion in germ cells. *Nucleic Acids Res.* 23:5080–5081.
- Sekine K, Kubo K, Nakajima K. 2014. How does Reelin control neuronal migration and layer formation in the developing mammalian neocortex? *Neurosci Res.* 86:50–58.
- Seri B, Garcia-Verdugo JM, McEwen BS, Alvarez-Buylla A. 2001. Astrocytes give rise to new neurons in the adult mammalian hippocampus. *J Neurosci.* 21:7153–7160.
- Sibbe M, Kuner E, Althof D, Frotscher M. 2015. Stem- and progenitor cell proliferation in the dentate gyrus of the Reeler mouse. *PLoS One.* 10:e0119643.
- Simeone A, Acampora D, Pannese M, D'Esposito M, Stornaiuolo A, Gulisano M, Mallamaci A, Kastury K, Druck T, Huebner K et al. 1994. Cloning and characterization of two members of the vertebrate dlx gene family. *Proc Natl Acad Sci U S A.* 91:2250–2254.
- Stanfield BB, Cowan WM. 1979. The development of the hippocampus and dentate gyrus in normal and Reeler mice. *J Comp Neurol.* 185:423–459.
- Steiner B, Kronenberg G, Jessberger S, Brandt MD, Reuter K, Kempermann G. 2004. Differential regulation of gliogenesis in the context of adult hippocampal neurogenesis in mice. *Glia.* 46:41–52.
- Stolp HB, Molnar Z. 2015. Neurogenic niches in the brain: help and hindrance of the barrier systems. *Front Neurosci.* 9:20.
- Takiguchi-Hayashi K, Sekiguchi M, Ashigaki S, Takamatsu M, Hasegawa H, Suzuki-Migishima R, Yokoyama M, Nakanishi S, Tanabe Y. 2004. Generation of Reelin-positive marginal zone cells from the caudomedial wall of telencephalic vesicles. *J Neurosci.* 24:2286–2295.
- Tan K, Duquette M, Liu JH, Lawler J, Wang JH. 2008. The crystal structure of the heparin-binding Reelin-N domain of f-spondin. *J Mol Biol.* 381:1213–1223.
- Tasic B, Yao Z, Graybuck LT, Smith KA, Nguyen TN, Bertagnolli D, Goldy J, Garren E, Economo MN, Viswanathan S et al. 2018. Shared and distinct transcriptomic cell types across neocortical areas. *Nature.* 563:72–78.
- Tinnes S, Ringwald J, Haas CA. 2013. TIMP-1 inhibits the proteolytic processing of Reelin in experimental epilepsy. *FASEB J.* 27:2542–2552.
- Tissir F, Goffinet AM. 2003. Reelin and brain development. *Nat Rev Neurosci.* 4:496–505.
- Trotter JH, Lussier AL, Psilos KE, Mahoney HL, Sponaugle AE, Hoe HS, Rebeck GW, Weeber EJ. 2014. Extracellular proteolysis of Reelin by tissue plasminogen activator following synaptic potentiation. *Neuroscience.* 274:299–307.

- Tueting P, Costa E, Dwivedi Y, Guidotti A, Impagnatiello F, Manev R, Pesold C. 1999. The phenotypic characteristics of heterozygous Reeler mouse. *Neuroreport*. 10:1329–1334.
- Utsunomiya-Tate N, Kubo K, Tate S, Kainosho M, Katayama E, Nakajima K, Mikoshiba K. 2000. Reelin molecules assemble together to form a large protein complex, which is inhibited by the function-blocking CR-50 antibody. *Proc Natl Acad Sci U S A*. 97:9729–9734.
- Wagener RJ, Witte M, Guy J, Mingo-Moreno N, Kugler S, Staiger JF. 2016. Thalamocortical connections drive intracortical activation of functional columns in the Mislaminated Reeler somatosensory cortex. *Cereb Cortex*. 26:820–837.
- Weeber EJ, Beffert U, Jones C, Christian JM, Förster E, Sweatt JD, Herz J. 2002. Reelin and ApoE receptors cooperate to enhance hippocampal synaptic plasticity and learning. *J Biol Chem*. 277:39944–39952.
- Weiss KH, Johanssen C, Tielsch A, Herz J, Deller T, Frotscher M, Förster E. 2003. Malformation of the radial glial scaffold in the dentate gyrus of Reeler mice, scrambler mice, and ApoER2/VLDLR-deficient mice. *J Comp Neurol*. 460:56–65.
- Won SJ, Kim SH, Xie L, Wang Y, Mao XO, Jin K, Greenberg DA. 2006. Reelin-deficient mice show impaired neurogenesis and increased stroke size. *Exp Neurol*. 198:250–259.
- Yasui N, Nogi T, Kitao T, Nakano Y, Hattori M, Takagi J. 2007. Structure of a receptor-binding fragment of Reelin and mutational analysis reveal a recognition mechanism similar to endocytic receptors. *Proc Natl Acad Sci U S A*. 104:9988–9993.
- Zhang WN, Bast T, Xu Y, Feldon J. 2014. Temporary inhibition of dorsal or ventral hippocampus by muscimol: distinct effects on measures of innate anxiety on the elevated plus maze, but similar disruption of contextual fear conditioning. *Behav Brain Res*. 262:47–56.
- Zhao S, Chai X, Frotscher M. 2007. Balance between neurogenesis and gliogenesis in the adult hippocampus: role for Reelin. *Dev Neurosci*. 29:84–90.